

# Interior Insulation of Mass Masonry Walls: Joist Monitoring, Material Test Optimization, Salt Effects

Building America Report - 1307

May 2013

Kohta Ueno, Randy Van Straaten and Chris Schumacher

---

Abstract:

*There are many existing buildings with load-bearing mass masonry walls, whose energy performance could be improved with the retrofit of insulation. However, adding insulation to the interior side of walls of such masonry buildings in cold climates may cause performance and durability problems. Some concerns have known solutions, but there are known knowledge gaps. Four topics were studied in more detail to address these gaps: the topics included moisture risks to embedded wood members, an examination of frost dilatometry test results for data patterns, the effect of dissolved salts on masonry durability, and optimization of the methodology of frost dilatometry testing.*

---

# Interior Insulation of Mass Masonry Walls: Joist Monitoring, Material Test Optimization, Salt Effects

K. Ueno, R. Van Straaten, C. Schumacher  
*Building Science Corporation*  
May 2013

## NOTICE

This report was prepared as an account of work sponsored by an agency of the United States government. Neither the United States government nor any agency thereof, nor any of their employees, subcontractors, or affiliated partners makes any warranty, express or implied, or assumes any legal liability or responsibility for the accuracy, completeness, or usefulness of any information, apparatus, product, or process disclosed, or represents that its use would not infringe privately owned rights. Reference herein to any specific commercial product, process, or service by trade name, trademark, manufacturer, or otherwise does not necessarily constitute or imply its endorsement, recommendation, or favoring by the United States government or any agency thereof. The views and opinions of authors expressed herein do not necessarily state or reflect those of the United States government or any agency thereof.

Available electronically at <http://www.osti.gov/bridge>

Available for a processing fee to U.S. Department of Energy  
and its contractors, in paper, from:

U.S. Department of Energy  
Office of Scientific and Technical Information  
P.O. Box 62  
Oak Ridge, TN 37831-0062  
phone: 865.576.8401  
fax: 865.576.5728

email: <mailto:reports@adonis.osti.gov>

Available for sale to the public, in paper, from:

U.S. Department of Commerce  
National Technical Information Service  
5285 Port Royal Road  
Springfield, VA 22161  
phone: 800.553.6847  
fax: 703.605.6900

email: [orders@ntis.fedworld.gov](mailto:orders@ntis.fedworld.gov)

online ordering: <http://www.ntis.gov/ordering.htm>



## **TO 3: 7.4.3 Interior Insulation of Mass Masonry Walls: Joist Monitoring, Material Test Optimization, Salt Effects**

Prepared for:

The National Renewable Energy Laboratory

On behalf of the U.S. Department of Energy's Building America Program

Office of Energy Efficiency and Renewable Energy

15013 Denver West Parkway

Golden, CO 80401

NREL Contract No. DE-AC36-08GO28308

Prepared by:

K. Ueno, R. Van Straaten, C. Schumacher

Building Science Corporation

30 Forest Street

Somerville, MA 02143

NREL Technical Monitor: Cheryn Metzger

Prepared under Subcontract No. KNDJ-0-40337-00

May 2013

**[This page left blank]**

## Contents

List of Figures .....	vii
List of Tables .....	ix
Definitions.....	x
Executive Summary .....	xi
<b>1 Introduction.....</b>	<b>1</b>
Background and Previous Work .....	1
Relevance to Building America’s Goals.....	2
Cost-Effectiveness .....	3
Tradeoffs and Other Benefits.....	4
Research Topics and Research Questions.....	4
Field Monitoring of Embedded Wood Members in Insulated Masonry Walls .....	4
Use of General Masonry Characteristics and Basic Materials Testing.....	4
Effect of Salts on the Durability of Masonry Materials.....	5
Optimization of Freeze Thaw Dilatometry Testing.....	5
<b>2 Field Monitoring of Embedded Wood Members in Insulated Masonry Walls .....</b>	<b>7</b>
Background.....	7
Literature Review.....	7
Experimental Design and Sensor Installation.....	9
Monitoring Overview.....	9
Building Monitoring Locations.....	13
Joist Sensors Package .....	19
Additional Sensors & Data Collection Logistics.....	22
Results to Date .....	24
Data Overview and Boundary Conditions .....	24
Joist Moisture Content Measurements: Unheated Wing Basement.....	26
Joist Moisture Content Measurements: Unheated Wing First Floor .....	29
Joist Moisture Content Measurements: Heated Wing Basement.....	31
Conclusions and Further Work .....	34
Analysis and Interpretation .....	34
Further Work.....	36
<b>3 Use of General Masonry Characteristics and Basic Materials Testing.....</b>	<b>37</b>
Introduction.....	37
Existing Material Property Data .....	38
Sample Dataset.....	39
Dry Density.....	40
Porosity .....	41
Water Uptake Coefficient .....	42
Free Water Saturation .....	43
Critical Degree of Saturation .....	44
Conclusions and Further Work .....	46
<b>4 Effect of Salts on the Durability of Masonry Materials .....</b>	<b>47</b>
Background.....	47
Salt and Freeze Thaw Damage .....	49
Salt Damage.....	51
Moisture Transport and Storage.....	52
Conclusions.....	52

<b>5</b>	<b>Optimization of Freeze Thaw Dilatometry Testing</b> .....	<b>54</b>
	Introduction.....	54
	Reduced Sample Sizes .....	54
	Sample Length Measurement .....	55
	Freeze-Thaw Cycle Time Improvement .....	60
<b>6</b>	<b>Research Question Answers and Further Work</b> .....	<b>65</b>
	Field Monitoring of Embedded Wood Members in Insulated Masonry Walls .....	65
	Use of General Masonry Characteristics and Basic Materials Testing.....	66
	Effect of Salts on the Durability of Masonry Materials.....	66
	Optimization of Freeze Thaw Dilatometry Testing .....	67
	Further Work.....	68
	Field Monitoring of Embedded Wood Members in Insulated Masonry Walls .....	68
	Use of General Masonry Characteristics and Basic Materials Testing.....	69
	Effect of Salts on the Durability of Masonry Materials.....	69
	Optimization of Freeze Thaw Dilatometry Testing .....	69
	<b>References</b> .....	<b>70</b>

## List of Figures

Figure 1: Merrimack Valley Habitat for Humanity retrofit building, Lawrence, MA.....	9
Figure 2: Overhead view of retrofit building from north (left) and west (right) .....	9
Figure 3: Exterior wall conditions at solid brick (left) and hollow clay block infill (right) conditions	10
Figure 4: Wall section at solid brick (left) and at hollow clay block infill (right) conditions .....	11
Figure 5: Multiple layers of insulation (left) and framing installed inboard of insulation (right).....	11
Figure 6: Embedded joist foam blocks (left); close-up showing clamping jig (right).....	12
Figure 7: Unit-to-unit floor/ceiling assembly at exterior wall; joists perpendicular to wall .....	12
Figure 8: Comparison of insulation strategies for joist ends BSMT-N-1/2/3, pre-drywall .....	13
Figure 9: Infrared comparison of BSMT-N1/N2/N3 joist ends (interior unheated) .....	14
Figure 10: BSMT-E-2 joist, showing existing water staining .....	14
Figure 11: BSMT-W1 and BSMT-W2 joists, showing water deposition at wall jog .....	15
Figure 12: FIRST-N joists, showing brick and clay block wall construction .....	15
Figure 13: Wood color comparison at BSMT-E-1 and FIRST-E joists .....	16
Figure 14: Two-component spray foam air seal at joists BSMT-W1 and BSMT-E1 .....	16
Figure 15: Location of monitored joist ends at basement level (basement ceiling); residential units highlighted .....	17
Figure 16: Location of monitored joist ends at first floor (first floor ceiling); residential units highlighted .....	18
Figure 17: Schematic of typical joist end sensor monitoring package .....	19
Figure 18: 6” extended moisture content pins (left) and determining drilling depth (right) .....	20
Figure 19: Pocket hole jig (left) and installed moisture content pins (right) .....	21
Figure 20: Caulked pocket holes (left) and air seal at joist pocket (right) .....	21
Figure 21: Installation of pocket RH sensor (left) and installed RH sensor (right) .....	22
Figure 22: Conditions in joist pocket at north-facing building at addition .....	22
Figure 23: Exterior (left) and interior hallway (right) temperature/relative humidity sensors .....	23
Figure 24: Data acquisition system, showing placement (left) and wiring connections (right) .....	23
Figure 25: Interior and exterior temperatures (Lawrence/KLWM airport data for comparison) .....	24
Figure 26: Interior and exterior relative humidity measurements (KLWM data for comparison) .....	25
Figure 27: Interior and exterior dewpoint temperatures (KLWM data for comparison).....	25
Figure 28: Basement unheated wing joist end measurements highlighted .....	26
Figure 29: Basement North 1 (insulated) joist end moisture contents and relative humidity .....	26
Figure 30: Basement North 2 (fiberglass) joist end moisture contents and relative humidity .....	27
Figure 31: Basement North 3 (uninsulated) joist end moisture contents and relative humidity .....	27
Figure 32: Basement East 2 joist end moisture contents and relative humidity.....	28
Figure 33: Basement South joist end moisture contents and relative humidity .....	29
Figure 34: Basement North and South joist pocket temperature comparison.....	29
Figure 35: First floor unheated wing joist end measurements highlighted .....	30
Figure 36: First North joist end moisture contents and relative humidity .....	30
Figure 37: First East joist end moisture contents and relative humidity .....	31
Figure 38: First South joist end moisture contents and relative humidity .....	31
Figure 39: Basement heated wing joist end measurements highlighted.....	32
Figure 40: Basement East-1 joist end moisture contents and relative humidity .....	32
Figure 41: Basement West-1 joist end moisture contents and relative humidity .....	33
Figure 42: First West-2 joist end moisture contents and relative humidity .....	33
Figure 43: First East joist end moisture contents and relative humidity .....	34
Figure 44: WUFI Layer/Material data .....	39
Figure 45: Sample set legend .....	39
Figure 46: Dry density vs. Vintage .....	40
Figure 47: Vacuum saturation vs. Vintage .....	41
Figure 48: Highly porous c. 1917 (left) and less porous c. 1940 (right) brick samples .....	41
Figure 49: Water uptake coefficient vs. Vintage .....	42
Figure 50: Free water saturation vs. Vintage .....	43
Figure 51: Critical degree of saturation vs. Vintage.....	44

---

**Figure 52: Critical degree of saturation as a fraction of Free Water Saturation vs. Vintage ..... 45**  
**Figure 53: Suspected de-icer salt damage (left) and basement capillary rise damage (right) ..... 47**  
**Figure 54: Brick spalling and paint blow-off basement party wall due to capillary rise ..... 48**  
**Figure 55: Capillarity (“rising damp”) transport of salts, causing efflorescence (Lstiburek 2007b) 48**  
**Figure 56: New (top) and old (bottom) brick slice samples ..... 55**  
**Figure 57: Freeze thaw testing results for New England circa 1900 brick samples ..... 56**  
**Figure 58: Photo and illustration of sample brick slice with metal screw targets ..... 56**  
**Figure 59: Strain measurements with (right) and without jig (left) ..... 57**  
**Figure 60: Average measurement decay over 5 consecutive measurements for 5 slices on one  
 'soft' brick sample ..... 58**  
**Figure 61: Average microstrain measurements of 5 'soft' brick slices after soaking in water for 1  
 hour relative to dry length (no freeze thaw cycles)..... 59**  
**Figure 62: Chilled bath (Schumacher 2011) ..... 61**  
**Figure 63: Sample 1 - Permanent microstrain measured after 15 freeze thaw cycles..... 61**  
**Figure 64: Sample 2 - Permanent microstrain measured after 15 freeze thaw cycles..... 62**  
**Figure 65: Sample 3 - Permanent microstrain measured after 15 freeze thaw cycles..... 62**  
**Figure 66: Freeze thaw testing typical cycling time ..... 63**  
**Figure 67: Thermistor installed within brick slice ..... 63**  
**Figure 68: Measured slice core temperature with initial and modified cycling routine ..... 64**

Unless otherwise noted, all figures were created by Building Science Corporation.

## List of Tables

<b>Table 1: Repeated length measurements (inches) of brick slices without jig.....</b>	<b>57</b>
<b>Table 2: Repeated length measurements (inches) of brick slices with jig .....</b>	<b>58</b>
<b>Table 3: Repeatability measurement (inches) after addressing ‘soft’ brick issue.....</b>	<b>60</b>

Unless otherwise noted, all tables were created by Building Science Corporation.

## Definitions

ASHRAE	American Society of Heating, Refrigerating and Air-Conditioning Engineers, Inc.
ASTM	American Society for Testing and Materials
BA	Building America Program
BSC	Building Science Corporation
ccSPF	Closed-cell Spray Polyurethane Foam
DOE	U.S. Department of Energy
DP	Dewpoint temperature
F-T	Freeze-thaw
ICC	International Code Council
IECC	International Energy Conservation Code
KLWM	Lawrence, MA Municipal Airport (weather station)
MC	Moisture content (wood % by weight)
MPa	Megapascal (1 MPa = 10 <sup>6</sup> Pascal)
μ-strain	Microstrain (one part per million, 10 <sup>-6</sup> )
MVHfH	Merrimack Valley Habitat for Humanity
NREL	National Renewable Energy Laboratory
RH	Relative humidity
S <sub>crit</sub>	Critical degree of saturation; see Mensinga et al. 2010
SPF	Spray Polyurethane Foam
STC	Building America Standing Technical Committee
WUFI	Wärme- Und Feuchtetransport Instationär
XPS	Extruded polystyrene

## Executive Summary

Load-bearing brick masonry buildings are a significant portion of the existing building stock; however, adding insulation to the interior side of walls of such masonry buildings in cold (and particularly cold and wet) climates may cause performance and durability problems in some cases. Previous work has helped disseminate information to North American practitioners on the durability risks associated these retrofits, and measures that can be taken to address these risks. However, there are known knowledge gaps; some topics are covered in the current report:

- Field monitoring of the hygrothermal behavior of moisture-sensitive wood beams embedded in a mass masonry structure retrofitted with interior insulation.
- Analysis of the existing database of masonry material property testing results, to determine whether freeze-thaw resistance generalizations can be made based on easily discernible properties.
- Examination of the effect of dissolved salts on freeze-thaw resistance of masonry materials, and determination whether test methods should be modified due to the presence of salts.
- Optimization of the testing of freeze-thaw resistance of masonry material samples, which included improvements in test repeatability, and reduction in test cycle time.

**Field Monitoring of Embedded Wood Members in Insulated Masonry Walls:** Wood members embedded in a masonry structure will be colder (and potentially wetter) after an interior insulation retrofit; the potential impact is not as well understood.

This work involves the field monitoring of embedded wood joist ends in a solid brick building which is being retrofitted with interior insulation. Eleven joists scattered throughout the building are being monitored, with a variety of orientations, exposures, and masonry wall types. The joists are being monitored for wood moisture content (low and high at the joist end), and temperature and relative humidity within the joist pocket. In addition, indoor and outdoor conditions are being recorded. Results have been collected for five months (December 2012-May 2013); one limitation of these preliminary results is that construction is still ongoing, and that the interior in much of the building is still at unheated and unoccupied conditions.

One conclusion was that the field monitoring methodology appears to provide valid and relevant data. Current results show that at many orientations (especially the north side of the building), joist moisture contents are high (20-30%), which reflects the long-term “mothballed” (unheated) condition of the building (past two winters). However, visual examination and installation of sensors revealed no signs of existing wood decay. On other, solar-heated orientations (south), the moisture content is in the safe, 10-13% range. The joist pocket relative humidity measurements match the patterns of wood moisture content measurements. The moisture contents at the joist “low” position (near the beam “seat”) are consistently higher than the corresponding “high” position. At the portion of the building that is heated, the joist ends dried rapidly after heating, even with the presence of interior insulation. However, air sealing and insulating the joist pockets resulted in increasing relative humidity and moisture contents.

This installation will continue to be monitored, as the building is completed and occupied, which will provide seasonal patterns (e.g., drying in summertime), as well as winter data from occupied conditions after construction completion.

**Use of General Masonry Characteristics and Basic Materials Testing:** Frost dilatometry (measurement of masonry critical degree of saturation/ $S_{crit}$ ) is used to assess freeze-thaw risks to masonry buildings retrofitted with interior thermal insulation. However, the associated testing and simulation activities add project cost and time requirements. Some practitioners have questioned whether frost dilatometry testing is required in every case, and whether generalizations could be made based on more easily obtained properties, such as manufacturer, manufacturing method (pressed vs. extruded brick), vintage, density, porosity, etc.

The database of 24 previous projects was analyzed to determine whether generalizations could be made, by plotting variables such as density, porosity, water uptake, and  $S_{crit}$  against vintage or other measurements. Few useful patterns could be discerned from this database. Further development of test methods and masonry material properties databases is recommended in the hope that future review of larger data sets may identify other opportunities for generalization.

**Effect of Salts on the Durability of Masonry Materials:** This research examined how salts affect the durability of masonry materials—and specifically, how they affect assessments of freeze thaw degradation risk when adding interior thermal insulation to masonry buildings. A literature search demonstrated that dissolved salts exacerbate freeze-thaw issues in concrete, and similar behavior is expected in masonry. These dissolved salts might influence frost dilatometry testing; this effect warrants further research. In addition, salt damage can occur by sub-efflorescence, or subfluorescence, where dissolved salts recrystallize within the pores below the masonry surface, and cause spalling due to the expansive force of crystal growth. Freeze-thaw and subfluorescence damage may be confused; determining salt content at damaged areas in the field is useful to understand the underlying mechanism. Furthermore, it is unclear if interior insulation retrofits can cause or exacerbate significant salt decay for walls, due to changes in temperature regime and/or drying magnitude or direction. Additional exploration is warranted.

**Optimization of Freeze Thaw Dilatometry Testing:** The frost dilatometry (freeze-thaw test) process often has to be repeated, and has significant time and cost requirements. Minimizing these time and cost obstacles would allow more thermal insulation retrofit projects to benefit from this testing. This work examined optimizations to testing methods, determining whether they had any detrimental effects on measurements.

Reducing the physical sample size allowed more samples to be fit into the chilled bath, doubling throughput. Sample length measurement was fine-tuned, switching from metal screw “targets” to a jig that ensured consistent placement of the sample and micrometer (without the use of targets). This reduced sample preparation time, and increased repeatability of measurements. Issues were found with length measurements of softer brick samples (sample erosion), and wet vs. dry measurements; protocols were improved to address these issues.

Freeze-thaw cycle time was reduced by almost half, by increasing the rate of cooling, decreasing the target thaw (upper) temperature, and decreasing the hold time from an hour to 30 minutes. These modifications could be made without any loss in accuracy in the test.

# 1 Introduction

Load-bearing brick masonry buildings are a significant portion of the existing building stock in the East Coast and Midwest regions of the United States. However, adding insulation to the interior side of walls of such masonry buildings in cold (and particularly cold and wet) climates may cause performance and durability problems in some cases. Exterior insulation provides the ideal conditions for building durability; however, many buildings cannot be retrofitted with insulation on the exterior for reasons such as historic preservation, cost, zoning or space restrictions, or aesthetics.

Previous Building America and other publications (Maurenbrecher and Shirtliffe 1998; Gonçalves 2003; Straube and Schumacher 2002, 2004, and 2007; BSC 2011; BSC 2012) have helped disseminate information to North American practitioners on the durability risks associated with interior insulation of masonry walls, and measures that can be taken to address these risks. However, there are known knowledge gaps in the body of literature, some of which are addressed in the current document. These research topics include the following items, and are covered in more detail under “Research Topics and Research Questions.”

- Field monitoring of the hygrothermal behavior of moisture-sensitive wood beams embedded in a mass masonry structure retrofitted with interior insulation.
- Analysis of the existing database of masonry material property testing results, to determine whether freeze-thaw resistance generalizations can be made based on easily discernible properties, such as vintage, geographic location, brick type (pressed vs. extruded), porosity, etc.
- Examination of the effect of dissolved salts on freeze-thaw resistance of masonry materials, and determination whether test methods should be modified due to the presence of salts.
- Optimization of the current regiment of masonry material property testing: in particular, determination of freeze-thaw resistance of samples. This optimization included improvements in test repeatability, and reduction in test cycle time requirements.

## Background and Previous Work

It is well established that exterior insulation provides the ideal conditions for building durability and performance (Hutcheon 1964); this approach is further described by Lstiburek (2007a). However, many buildings cannot be retrofitted with insulation on the exterior for reasons such as historic preservation, cost, zoning or space restrictions, or aesthetics.

Numerous obstacles to more wide-scale deployment of interior retrofits include concerns about freeze-thaw damage due to reduced outward heat flow and reduced inward drying, and the potential for decay of wood structural framing members (typically floor joists) that are embedded in mass assemblies. The problems and some case studies of interior retrofits are outlined by practitioners such as Maurenbrecher et al. (1998), Gonçalves (2003), and Straube and Schumacher (2002, 2004).

The masonry freeze-thaw issue has been examined by (among others) Litvan (1975a), Mensinga et al. (2010), and Lstiburek (2010). These practitioners propose the use of material property testing as an input to hygrothermal simulations, using a limit states design approach, where load (climate exposure) is compared with the capacity (freeze-thaw resistance of the brick). The embedded floor joist decay issue has been studied by some practitioners (Dumont et al. 2005, Scheffler 2009, Morelli 2010, Morelli and Svendsen 2012, Ueno 2012), but many issues remain unresolved.

Straube and Schumacher (2007) reviewed the moisture control principles that must be followed for a successful insulated retrofit of a solid load-bearing masonry wall. Interior insulation reduces heat flow through the assembly, thus changing the existing moisture balance of wetting and drying. Given this reduced drying, the retrofit design should reduce wetting in a commensurate manner. The winter temperatures of parts of the inner layers of masonry are also significantly lowered, thereby raising the risk of freeze-thaw damage. This document was intended for architectural practitioners.

Previous Building America work includes BSC TO2 Task 7.3: “Internal Insulation of Masonry Walls: Final Measure Guideline” (BSC 2012). This Measure Guideline presents the current knowledge in terms of moisture-safe retrofits of mass masonry walls, expanding on Straube and Schumacher (2007). It also includes a checklist intended as a brief outline of key points and takeaways, which can be used by a field practitioner when assessing a mass masonry building for interior insulation. The intention was that the Measure Guideline would provide more detailed explanations and visual examples of items covered in the checklist.

In addition, BSC led a Building America Experts Meeting on this topic, with contributions from multiple practitioners, and discussions on gaps in the current knowledge and recommendations for future work. A full report is provided in BSC Task 1.3: “Recommended Approaches to the Retrofit of Masonry Wall Assemblies: Final Expert Meeting Report” (BSC 2011).

### **Relevance to Building America’s Goals**

Given the Building America goals of reducing home energy use by 30%-50% (compared to 2009 energy codes for new homes and pre-retrofit energy use for existing homes), insulation and air sealing of mass masonry walls will need to be a component of the work if mass masonry residential buildings are to be addressed. Potentially millions of housing units could benefit from a better understanding of the moisture risks associated with interior retrofits, and the means of reducing these risks.

The majority of construction that can benefit from this research is in locations with older building stock (i.e., mass masonry). The greatest concentrations are likely on the East Coast and in the Midwest (i.e., cold climates), although these types of buildings are definitely present throughout the country.

One belief that appears to be common among less technical practitioners is that insulation of mass masonry structures is not possible (due to potential for damage) and/or unnecessary (as thermal mass effects provide sufficient benefits). Previous work discussed above covers risk management for interior insulation of mass masonry walls. Basic energy models can be used to show that uninsulated thermal mass does not result in significant improvement to energy

performance for buildings located in heating-dominated (cold) climates. Thermal mass is of greater benefit in locations with high diurnal swings around the interior setpoint, as commonly found in the United States Southwest. This is covered in more detail by BSC (2012). Note, however, that thermal mass is not dismissed as a concept: energy savings can be obtained by combining insulation with thermal mass (e.g., charging mass with passive solar gains). Temporal load shifting effects can be another benefit, such as pre-cooling of a meeting room to reduce peak load effects and minimize installed equipment size.

The research topics proposed here are specifically relevant based on the current needs of practitioners. The Building America Standing Technical Committee on Enclosures has identified both of these as important topics for additional research work (see Enclosures STC Strategic Plan: #30 Walls: Interior Masonry Retrofits; and #39 Walls: Embedded Wood Beams and Joists.)

### **Cost-Effectiveness**

Load bearing masonry has a wide range of thermal properties. However, even a ‘thick’ multi-wythe load-bearing masonry wall is likely to have an R-value in the range of R-3.2 to R-6.8, with an average R-value of around R-5. Surface heat transfer coefficients (“air films”) of another R-1 may result in thermal performance comparable to that of a high-end (i.e. triple glazed) modern window; however this level of insulation is too low for most practical purposes (considering current energy costs, building durability, health and thermal comfort issues). Hence insulation is often added during retrofits, and is critical to achieving high performance (as per Building America program goals) in any climate with significant heating loads.

The R-values of uninsulated masonry walls are also substantially below modern code requirements for cold climates: for Zones 5 and 6, the typical opaque-wall “true” R-value requirements are in the range of R-12 to R-17 (as calculated from U values given in the 2009 International Energy Conservation Code/IECC, Table 402.1.3; ICC 2009).

Thermal insulation follows the law of diminishing returns, with decreasing return on investment with increasing insulation thickness. Given that these wall assemblies are being changed from uninsulated (base case) to insulated (final) assemblies, it is likely that the initial inch or two of insulation should be highly cost-effective. Optimization would be a function of insulation cost, energy costs, and climate zone.

BSC’s current retrofit recommendations include the use of closed-cell air-impermeable spray foam as an interior insulation material for mass masonry walls. Closed-cell spray foam (ccSPF) has a typical installed price of roughly \$1.00 per board foot (although prices appear to be falling below this level); when normalized by R value (instead of volume) this is equivalent to approximately \$0.16/sf·R. In comparison, typical loose-fill fibrous insulations are sold at \$0.02-0.04/sf·R; note that this is a material cost, not an installed cost. If a 1:1 material-to-installation cost ratio is assumed for this estimate, the use of closed-cell spray foam is still roughly two to four times as expensive as the lowest-cost loose fill materials. However, as discussed by Straube and Schumacher (2007) and BSC (2012), the use of air permeable, moisture-sensitive fibrous insulations in this application results in assemblies with higher risk of moisture-related failures.

## **Tradeoffs and Other Benefits**

Basic benefits of the retrofit insulation of uninsulated masonry walls include energy savings and thermal comfort improvements for occupants (due to radiant surface temperature effects and air leakage reduction). The assemblies under discussion could meet requirements for modern energy codes, as discussed earlier, unlike the non-retrofitted assemblies.

## **Research Topics and Research Questions**

The research topics and associated questions are broken down here by section; the answers to these research questions are provided in the conclusion of this report.

### ***Field Monitoring of Embedded Wood Members in Insulated Masonry Walls***

Previous simulation work on embedded wood members in insulated masonry walls left many open questions, which could be addressed—at least in part—by in-situ measurement of embedded member moisture content. This field testing was done in collaboration with Merrimack Valley Habitat for Humanity (MVHfH) in Lawrence, MA. This organization is currently in the process of renovating a mass masonry multi-family building into 10 condominium units; the monitoring equipment is installed at joists at this site. The associated research questions were as follows:

- What are the temperature conditions at the joist pockets or beam pockets with and without retrofitted interior insulation?
- What are the measured seasonal moisture contents of embedded beams in insulated and uninsulated cases, and can these be mapped to durability risks?
- Does orientation have a specific effect of temperature and moisture conditions? This will include both the effects of solar gain and wind-driven rain.
- Does distance from grade (and thus “rising damp,” via capillary activity) have a specific effect on temperature and moisture conditions?
- Is there a significant difference in the performance of an insulated beam without an air seal around the beam pocket, compared to one that is rigorously air sealed?
- Are there measurable airflows occurring at joist pockets in wintertime or summertime conditions? Given the limits of hot wire anemometers, it is unlikely that airflows are within the measurement range, but will be checked for reference.
- How do the monitored data correspond to previous three-dimensional and one-dimensional simulations?

### ***Use of General Masonry Characteristics and Basic Materials Testing***

Frost dilatometry is a costly and time-consuming test, which has probably limited its application to high profile and/or high value projects. If generalizations could be made on freeze-thaw resistance from variables such as brick vintage, type (pressed vs. extruded), manufacturer, porosity, or other easily recognizable physical characteristics, it would simplify risk assessments for interior insulation. BSC has collected a database of material properties from previous

projects, which can be compared with the variables described above. However, there is a great deal of variability in measurements; a larger sample set would be required to obtain robust and reliable results. The relevant research question is:

- Based on analysis of the existing database of masonry material property testing results, can freeze-thaw resistance generalizations be made based on easily discernible properties, such as vintage, geographic location, brick type (pressed vs. extruded), porosity, etc.?

### ***Effect of Salts on the Durability of Masonry Materials***

The issue of effect of salts (dissolved in mass masonry) on freeze-thaw behavior was raised at BSC's July 2011 Building America Experts Meeting (BSC 2011). Salts, acting alone, can cause damage to masonry materials (via subfluorescence); it is possible that visible damage may be due to this salt migration. In addition, the presence of dissolved salts can exacerbate freeze-thaw damage in masonry materials. The associated research questions were as follows:

- What is the theoretical impact of salts in masonry materials?
- How might dissolved salts affect the mechanics of freeze-thaw?
- What range of osmotic pressures (pressure drives due to different salt concentrations) might be expected? Could these pressures result in damage?
- What are the mechanics of subfluorescence?
- Do practitioners confuse freeze-thaw damage and salt damage in the field?

### ***Optimization of Freeze Thaw Dilatometry Testing***

As described previously, masonry material property testing (frost dilatometry) is a costly and time-consuming procedure. Further development is warranted to make it a more available, repeatable, and commonplace tool for practitioners. The research team has done work to optimize testing, such as improving the repeatability of dilatometry measurements, decreasing freeze-thaw cycle time, increasing precision in sample length measurement, and increased accuracy in interpretation of results. The associated research questions were as follows; they examined improving repeatability (in measuring the length of masonry samples), and improving test throughput (reducing cycle time from the current two day cycle).

- Can targets (metal reference points attached to the sample, similar to those used in structural testing) be used to improve repeatability of dimension measurements?
- Is there an alternative to measuring dimensions; for example, can freeze-thaw damage be identified via acoustic methods such as measurements of attenuation?
- Can the freeze-thaw cycle be modified in order to decrease test cycle time, and therefore increase throughput?
- Alternately, could the cycle time be compressed to allow more freeze-thaw cycles and a greater dilation to be achieved in a shorter time period?

- Are the temperatures & time steps currently used sufficient to bring the entire masonry specimen (including the core) to target temperatures?

## 2 Field Monitoring of Embedded Wood Members in Insulated Masonry Walls

Wood members embedded in a masonry structure will be colder (and potentially wetter) after an interior insulation retrofit; the potential impact is not as well understood. The work in this section involved the field monitoring of embedded wood joist ends in a solid brick building which is being retrofitted with interior insulation

### Background

There are durability risks and concerns when applying interior insulation to mass masonry walls. Some of them have been (or are being) addressed, including interstitial condensation and brick freeze-thaw damage. However, another durability risk that has received less investigation is the hygrothermal behavior of moisture-sensitive wood beams embedded in the load-bearing masonry. With the retrofit of interior insulation, the embedded beam ends will spend longer periods at colder temperatures than their pre-retrofit condition. Therefore, these wood members will have reduced drying potential due to reduced heat or energy flow (as described by Lstiburek 2008). The wood will also be subjected to higher relative humidity (RH) conditions in the beam pocket, and therefore remain at a higher moisture content (MC): both of these factors increase the risk to the beam's durability.

Some solutions that have been proposed and/or used to protect embedded members include borate preservative injections into the wood; metal plates next to the member (to provide passive heat flow); active heating at the beam ends; or construction of a load bearing structure inside the masonry, and cutting off the end of the beam.

### Literature Review

Several practitioners have examined the problem of moisture risks at embedded members, using both in-situ monitoring and simulations.

Dumont et al. (2005) monitored moisture content of wood structural members embedded in masonry in two low-rise residences that were retrofitted with insulation in Wolseley, SK (DOE Zone 7, "dry" climate) and Kincardine, ON (DOE Zone 6A, "moist" climate). The Wolseley house was insulated with mineral wool, with a polyethylene vapor barrier; the Kincardine house was insulated with spray polyurethane foam. The foam insulation encased the wood members where they were seated in the masonry wall.

Data showed that the wood members of the Wolseley house remained at safe moisture content levels (10-15%) throughout the monitoring period. This is not meant as an endorsement of the use of air-permeable insulation with an impermeable interior vapor barrier: this is actually a high risk assembly. However, the lack of moisture load (dry climate) is likely the dominant factor. In contrast, the Kincardine house showed consistently elevated moisture contents (20%+) at several locations. It was suspected that the moisture source was capillary uptake from the wet foundation, but rainwater absorption through the face of the masonry (due to surface detailing) was not eliminated as a possible source. The limited drying to the interior available through spray polyurethane foam was also likely a contributing factor.

Scheffler (2009) used simulations to examine the problem of moisture accumulation at wooden beam ends. He used DELPHIN two-dimensional hygrothermal simulation software, running a wooden beam embedded in brick masonry under steady state conditions (23° F/-5° C/80% RH exterior; 68° F/20° C/50% RH interior; 90 days). These simulations indicated the moisture risks associated with insufficient control of airflow or moisture vapor flow (diffusion) from interior sources. This was followed by one-dimensional and two-dimensional simulations using transient weather data (Bremen; mild, maritime climate with high rain and humidity), indicating increases in relative humidity and liquid water (condensation) at the beam ends due to the addition of insulation.

Scheffler also described the historic methods to increase embedded beam longevity, such as charring the beam end to increase moisture resistance, and the addition of exterior-to-interior ventilation at the beam pocket. He discussed current methods to ameliorate these moisture issues due to insulation retrofits, including replacement of wood floor/ceiling assemblies with non-moisture sensitive materials (e.g., concrete), and possibly the addition of heat and/or ventilation at the wood beam end.

Morelli et al. (2010) collaborated with Scheffler, continuing examinations of this issue. They proposed the solution of leaving a gap in the insulation of 12” (300mm) above and below the floor, resulting in a 30” (770 mm) gap (12” gap×2 plus floor depth). Two- and three-dimensional heat transfer simulation showed that the heat flow was reduced by 60% going from the uninsulated to insulated cases, while the “gap” case was only a 45% reduction. This work was followed by two-dimensional DELPHIN hygrothermal simulations of the embedded beam (in a Bremen climate). Relative humidity levels in a corner of the beam pocket (and equilibrium wood moisture content) were compared between cases. The existing, uninsulated wall showed a drying trend; the fully insulated wall showed seasonal increases in RH; and the gapped insulation wall showed performance between the two previous cases (but with increasing moisture levels). However, these results assumed a relatively high wind-driven rain loading factor. Switching to a lower loading factor resulted in the gapped insulation assembly showing a general drying trend.

Morelli and Svendsen (2012) continued the previous work of Morelli (2010), showing further simulations with continuous interior insulation, and insulation installed with a gap at the floor beams. Another result of this research was a methodology for assessing retrofit measures on brick masonry walls based on a failure mode and effect analysis.

Morelli and Svendsen also performed an extensive literature review from the 1980s to current day. Several in-situ field studies were examined; the typical findings were that driving rain did not result in moisture problems at beam ends. Some researchers found that cracks in the façade could result in problems, but crack-free façades had acceptable performance. Another researcher examined the effect of interior air leakage at beam ends: at high air leakage rates, temperatures in the beam pocket were increased, reducing condensation risks. At low air leakage rates, air-transported moisture was negligible. However, at intermediate flows, condensation did occur. That researcher recommended the addition of localized exterior wall insulation at beam ends, or insulating the beam end cavity. Other researchers examined techniques such as adding heat to the beam ends to avoid moisture problems. The results kept wood moisture contents low, but this is an expensive (and therefore unlikely) retrofit.

Ueno (2012) examined this problem by first using three dimensional heat flow simulations to determine embedded beam and joist end temperatures with and without interior insulation. Various mitigation techniques, such as heat flow plates or omitting insulation, were also simulated. These results were then used to inform one-dimensional hygrothermal simulations of embedded beam ends. These hygrothermal simulations gave inconclusive results; the author recommended a possible first step of using of two-dimensional hygrothermal simulations. However, greater and more defensible insight could be gained by in-situ measurements of beam pocket temperatures, relative humidity, and wood moisture content (in both insulated and uninsulated configurations, and various orientations and rainfall exposure levels).

Based on Ueno’s conclusions, this research project measured in-situ conditions of embedded wood joists in an interior insulated masonry structure.

## Experimental Design and Sensor Installation

### *Monitoring Overview*

This field monitoring work was done at an existing brick mass masonry building in Lawrence, MA, which is being renovated by the Merrimack Valley Habitat for Humanity (MVHfH) into ten condominium units (Figure 1).

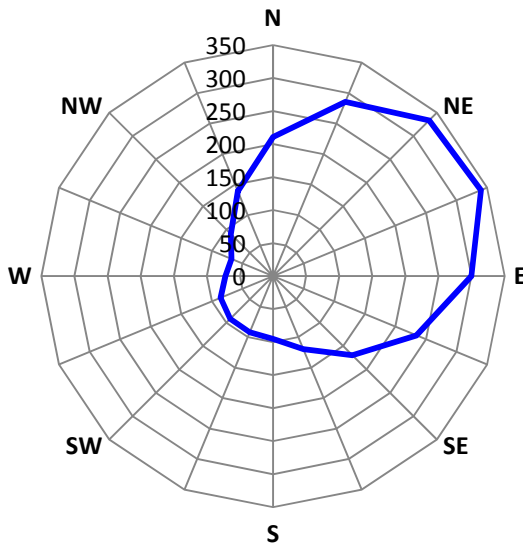


Figure 1: Merrimack Valley Habitat for Humanity retrofit building from west (left) and north (right)



Figure 2: Overhead view of retrofit building from west (left) and north (right)

The past year’s weather data (May 2012-May 2013) for the nearest station (Lawrence Municipal Airport/KLWM) was used to create a driving rain rosette (Figure 3), using methods described in Straube and Burnett (2005). It shows that the greatest driving rain deposition occurs on the rear face of the building (project East). There is some shielding of the building due to adjacent trees during non-winter conditions.



**Figure 3: Driving rain rosette for KLWM, rain in mm/year (left) and overhead view (right)**

The construction of the masonry walls at this project include both multi-wythe solid brick walls, and exterior brick with a hollow clay block infill/backup wall, as shown in Figure 4. These photos show conditions after demolition of the interior furring, lath, and plaster. Solid multi-wythe brick is used at the original portion of the building (west-facing front elevation; circa 1906 construction; see Figure 1, left); clay block is used at the east-facing rear addition (circa 1930 construction; Figure 1, right).



**Figure 4: Exterior wall conditions at solid brick (left) and hollow clay block infill (right) conditions**

Although these assemblies appear to be monolithic from the interior and exterior, there are a variety of interconnected spaces, such as the incompletely filled collar joints between brick wythes (Figure 5, left), or the hollow cores of the clay blocks (Figure 5, right).



**Figure 5: Wall section at solid brick (left) and at hollow clay block infill (right) conditions**

The building is being retrofitted with interior insulation, which consists of three 2” layers of extruded polystyrene (XPS) insulation adhered to the existing masonry with polyurethane adhesive (Figure 6, left). The seams are staggered, and are taped on the innermost and outermost layers, to improve air barrier performance. Wood 2x4 framing is installed inboard of the XPS insulation for mechanical systems and services (Figure 6, right); the cavity is left uninsulated.



**Figure 6: Multiple layers of insulation (left) and framing installed inboard of insulation (right)**

The embedded wood structure consists of dimension lumber (roughly 2” thickness) joists at a close spacing (16” on center typical), as opposed to large, widely-spaced timbers or beams. Typical conditions are shown in Figure 7 (left). The insulation approach at the embedded beams is to use scraps of rigid XPS foam insulation, installed with polyurethane adhesive. This approach consumes available scrap; note that there is a generous space at the perimeter of each block, which allows effective air sealing with a spray foam kit.



**Figure 7: Embedded joist foam blocks (left); close-up showing clamping jig (right)**

The typical floor-to-floor detail is shown in Figure 8, showing spray foam at the joist space. This floor-to-floor separation detail also needs to meet fire separation requirements, which is the reason for the discontinuities in the insulation (see “New strip of mold resistant fire-rated gypsum board”).

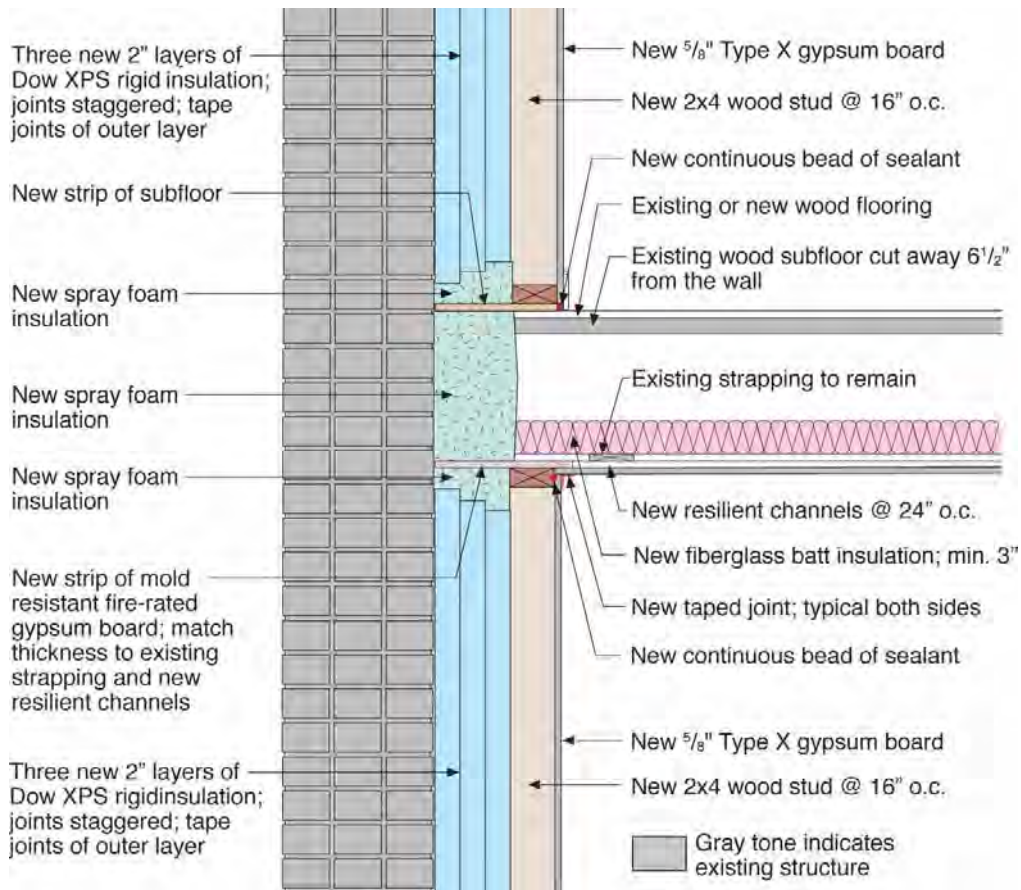


**Figure 8: Unit-to-unit floor/ceiling assembly at exterior wall; joists perpendicular to wall**

## **Building Monitoring Locations**

In order to capture a variety of conditions, joists were monitored in multiple locations throughout the building. Some variables of interest included cardinal orientations (and thus solar heating/drying, as well as wind-driven rain exposure), masonry wall type (solid brick masonry vs. hollow clay tile backup), localized wetting exposure, and insulation strategy. There are eleven monitored joist locations in total; the logic behind the joist selection is described in more detail below.

The monitored joists are located in the basement ceiling framing and the first floor ceiling framing; the layout is shown on the building plan in Figure 16 and Figure 17. The floor plans also show the footprints of the individual condominium units for reference. The monitoring package used at each joist is covered in detail in the following section.

As discussed earlier, the front/west wing of the building is original construction, with solid brick masonry walls. The rear/east wing of the building is an addition, with hollow clay block backup walls and a brick veneer. The separation between these two wall types is shown in Figure 17, for the first floor. However, the basement level walls are built with solid brick at both the original wing and the addition, likely for structural reasons.

The logic behind the selection of monitored joists is described in more detail as follows:

Basement ceiling joists (BSMT-[orientation][number]) are monitored on all four orientations (including multiple measurements on some orientation); all are embedded in solid brick masonry.

BSMT-N1/N2/N3 are joists with identical exposure, but using different retrofit strategies:

- BSMT-N1 is insulated as per the remainder of this project, insulated and air sealed with rigid foam and urethane spray foam
- BSMT-N2 is insulated with air-permeable insulation (two R-13 layers of fiberglass batt, or R-26), which captures the effect of insulating, while still allowing airflow.
- BSMT-N3 is left uninsulated, similar to assemblies described in Morelli's research (2010).



**Figure 9: Comparison of insulation strategies for joist ends BSMT-N-1/2/3, pre-drywall**

These test joists are specifically located in a building common area; therefore, if monitoring indicates that one of these strategies results in excess moisture accumulation, the finish ceiling (gypsum board) can be opened, and the poor performer will be retrofitted with another strategy.

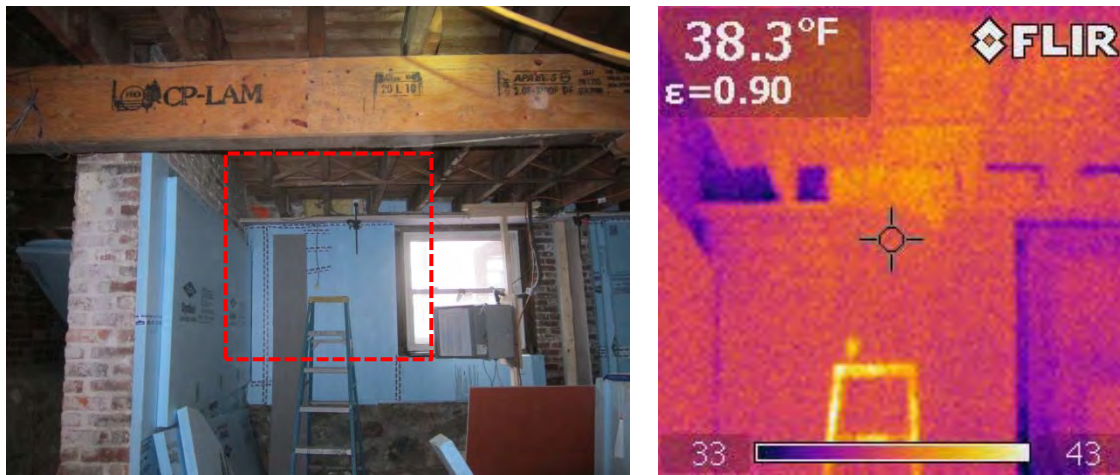


**Figure 10: Infrared comparison of BSMT-N1/N2/N3 joist ends (interior unheated)**

BSMT-E2 is of particular interest because it shows evidence of previous water penetration (staining of the beam end). The east orientation at the rear of the building also has the highest exposure for driving rain. It is unknown whether these bulk water issues have been solved in previous renovations, or if there might be some unknown hidden leakage path.



**Figure 11: BSMT-E-2 joist, showing existing water staining**

BSMT-W1 and BSMT-W2 are of interest because during the site inspection, it was noted that rainwater was being deposited on the wall at the “jog.” BSMT-W1 was set up to capture the mostly-dry field of the wall, while BSMT-W2 was located close to the jog, to determine whether this bulk water was sufficient to cause issues with the embedded joist end moisture behavior. This orientation has low driving rain exposure.



**Figure 12: BSMT-W1 and BSMT-W2 joists, showing water deposition at wall jog**

BSMT-S1 is of some interest because hygrothermal simulation work (Ueno 2012) seemed to indicate that south-facing embedded wood members would be vulnerable to moisture accumulation due to summertime inward vapor drives. Whether this effect occurs (and the magnitude of the effect, if it occurs) will be studied by comparing behavior on different solar orientations.

On the first floor, joists were only monitored in the addition (hollow clay block) walls, due to a lack of access to joists in the first floor original wing. The hollow clay block backup walls are actually constructed with alternating layers of block and brick, as shown in Figure 13, which shows the FIRST-N monitoring locations.



**Figure 13: FIRST-N joists, showing brick and clay block wall construction**

Monitoring was installed in north, south, and east-facing joists. The east-facing joist appears to be a different species: the wood is noticeably softer, and is a different color (see Figure 14). This difference in wood species may have an effect on moisture content measurements via electrical resistance.



**Figure 14: Wood color comparison at BSMT-E-1 and FIRST-E joists**

The insulation blocks have been installed between the floor joists at the front (west) wing, which contains BSMT-W1, BSMT-W2, and BSMT-E1. These joists have been insulated and air sealed to the perimeter of the foam blocks with a two-component spray foam pack, as shown in Figure 15. The remaining joists are running at close to ambient conditions, and have not yet been insulated.



**Figure 15: Two-component spray foam air seal at joists BSMT-W1 and BSMT-E1**

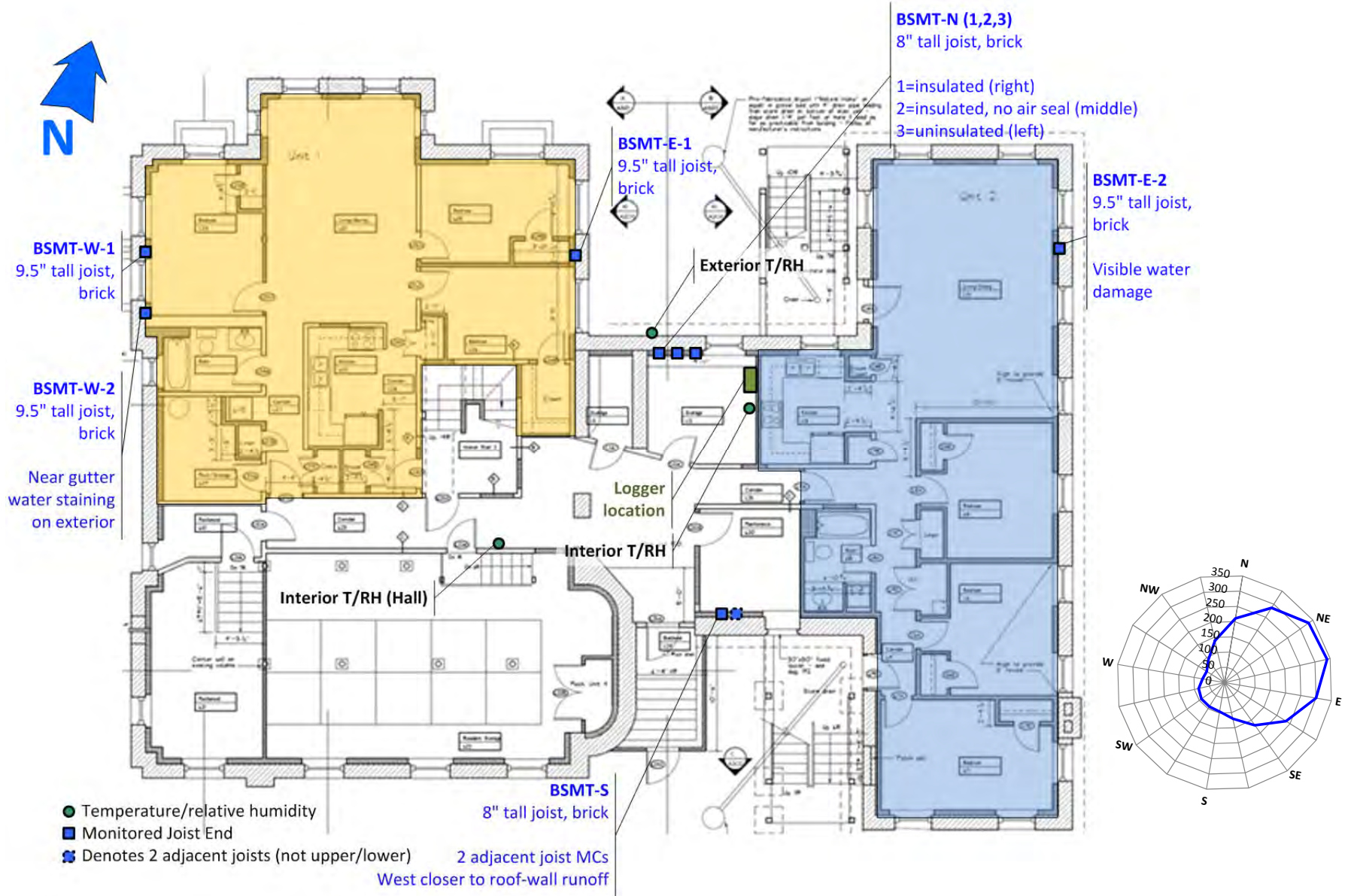


Figure 16: Location of monitored joist ends at basement level (basement ceiling), with driving rain; residential units highlighted

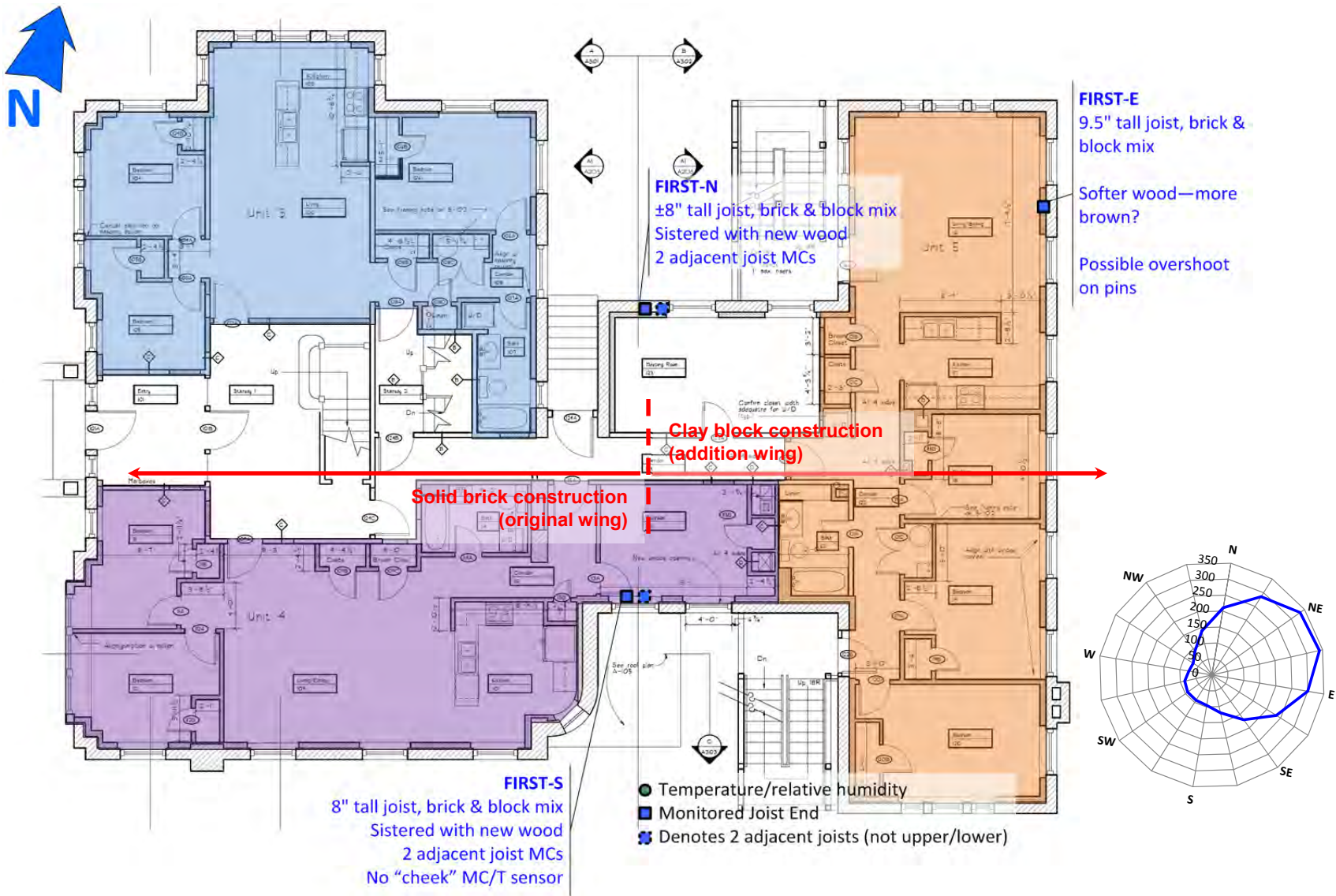


Figure 17: Location of monitored joist ends at first floor (first floor ceiling), with driving rain; residential units highlighted

### Joist Sensors Package

Three types of sensors are used to monitor conditions within the assembly:

- Temperature sensors (10k NTC thermistors (accuracy  $\pm 0.2^{\circ}\text{C}$ )
- Relative humidity (RH) sensors (thermoset polymer capacitive based sensors with onboard signal conditioning (accuracy  $\pm 3\%$  between 10 & 90% RH)
- Wood Moisture Content (MC) (in-situ electrical based resistance measurements between corrosion resistant insulated pins)

The specifics of these sensors are covered in detail by Straube et al. (2002). The sensor package installed at each joist is shown schematically in Figure 18. Note that the ends of the joists are “fire cut,” or cut at an angle so that a fire which burns through a joist will not collapse the masonry wall by “levering” the structure upward and outward.

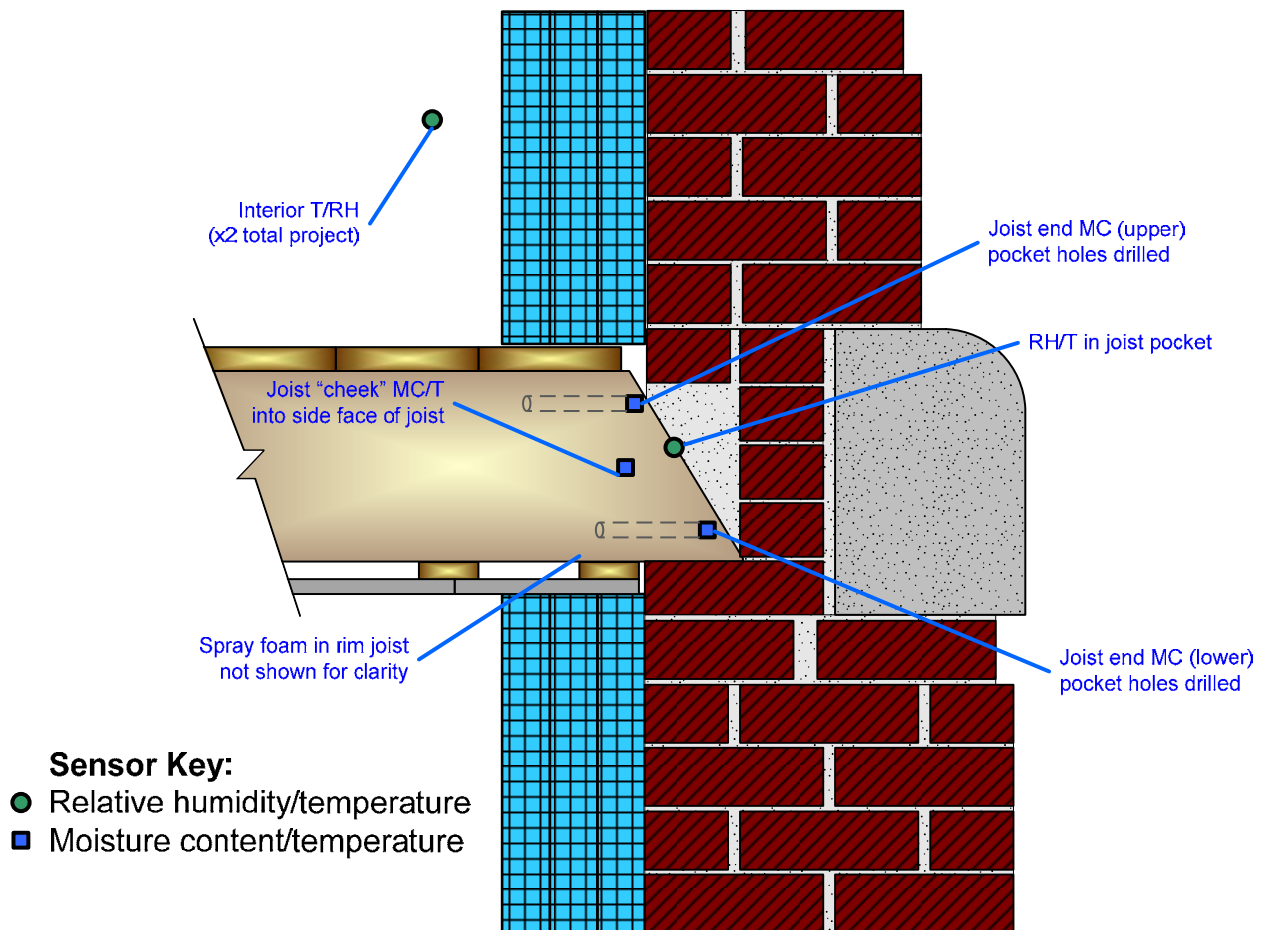


**Figure 18: Schematic of typical joist end sensor monitoring package**

- The moisture content at the embedded end of the joist is monitored by two sets of extended electrical resistance pins, which are driven from the interior side through pilot holes. Moisture contents are typically measured at low and high locations in each joist end. This is intended to capture whether or not moisture contents are higher where the

joist is seated into (and in direct contact with) the mortar and masonry walls. The pins are driven to measure moisture content at the outermost 1” of the beam.

- In some cases, the upper sensor was omitted, because the upper location was not embedded in the masonry. In those cases, two “lower” moisture content sensors were installed in adjacent beams. These cases are noted in the description of sensor locations in Figure 16 and Figure 17; this was done at BMST-S, FIRST-N, and FIRST-S.
- The side face or “cheek” of the joist is also measured for moisture content and temperature. This was done primarily as a reference check: it provides a third reference point for moisture content measurement anomalies, which might be due to wood species differences. In addition, it provides a limited amount of spatial resolution: it might indicate the extent of moisture migration, when the deeply embedded end of a joist shows high moisture contents. This “cheek” location is typically concealed within the interior insulation after the installation of spray foam.
- A temperature and relative humidity sensor is installed within the “pocket” where the joist is embedded in the masonry wall. Installation of this sensor was not necessarily consistent, as many of these joists were grouted in place with mortar, with a limited air gap. Other joists had a distinct air gap. A lack of an air gap increases the vulnerability of an embedded wood member, as the wood is in direct capillary contact with the moisture-absorbent masonry on the sides (as well as the bottom).

No capillary break is installed on the underside of the joist, at its “seat” in the wall. This stands in contrast to the practice used for larger timber beams, of using a steel or cast iron bearing plate. This plate is used primarily for structural reasons, but it also acts as a capillary break.

The joist ends were monitored using 6” long sharpened stainless steel pins attached to wire leads, as shown in Figure 19 (left). First, the end of the joist was examined, to determine the angle of its fire cut, and the location of the end of the joist (Figure 19 right).



**Figure 19: 6” extended moisture content pins (left) and determining drilling depth (right)**

Then, a pilot hole was drilled at an shallow angle in the beam, using a pocket hole jig (Figure 20). A 1/8” diameter hole was drilled for clearance for the pin, but the joist end was left

undisturbed, so that the pin would be driven directly into wood fibers with frictional contact. Figure 20 (right) shows the upper and lower joist end moisture content measurements and the “cheek” moisture content/temperature measurement.



**Figure 20: Pocket hole jig (left) and installed moisture content pins (right)**

The pocket holes for the joist end moisture contents were sealed from interior air and water vapor with a vapor-impermeable synthetic rubber caulk (Figure 21 left). The joist pockets were air sealed from the interior with a combination of can-based expanding foam (Figure 21), and the spray foam kit used around the rigid blocks of foam mentioned earlier (Figure 15).



**Figure 21: Caulked pocket holes (left) and air seal at joist pocket (right)**

The temperature and relative humidity sensors were installed at any air space available between the joist and the masonry. In some cases, space was readily available to insert the sensor, as shown in Figure 22. In other cases, some demolition of the mortar around the beam was required to install the sensor.



**Figure 22: Installation of pocket RH sensor (left) and installed RH sensor (right)**

The condition of the masonry joist pocket could be observed directly at several north-facing openings in the addition portion of the building, where a beam had been removed (Figure 23). It appears that mortar or grout was packed in between the brick and the wood joist during installation; in addition, mortar was packed in at the angled space behind the fire cut. However, at the hollow clay block, there would be an air space adjacent to the joist, which would likely increase drying.



**Figure 23: Conditions in joist pocket at north-facing building at addition**

### ***Additional Sensors & Data Collection Logistics***

Interior temperature and relative humidity conditions are measured at two locations, as shown in Figure 16. One interior T/RH measurement is directly below the data acquisition system (data logger), and the other is in the common hallway at the front of the building (Figure 24, right), both on the basement level. The basement level was chosen because the majority of the sensors are located on this floor. In addition, the front of the building is currently heated with temporary construction heat, while the rear portion is operating near ambient conditions. The two interior sensors measure these two disparate conditions.

An exterior temperature and relative humidity sensor (Campbell Scientific HMP60 Temperature and Relative Humidity probe; Figure 24, left) provides outdoor conditions synchronized to the

joist end measurements; it is located within a solar radiation shield on the north side ground floor of the building. Additional outdoor weather conditions (including precipitation, and wind speed and direction) are being collected from online sources for comparison; the nearest weather station is Lawrence Municipal Airport (KLWM).



**Figure 24: Exterior (left) and interior hallway (right) temperature/relative humidity sensors**

Data are being collected by a Campbell Scientific CR1000 measurement and control system, installed in a basement storage room (Figure 25). Extension cables were run from the sensor locations to the data collection system before the application of interior finishes. Data are being measured at five minute intervals, and average values are recorded hourly. No battery backup for the data logger is provided; however, the unit has non-volatile memory, and will resume data collection after a power failure. Data will be downloaded during site visits, by direct connection (as opposed to remote downloads).



**Figure 25: Data acquisition system, showing placement (left) and wiring connections (right)**

## Results to Date

### ***Data Overview and Boundary Conditions***

Data have been collected from mid-December 2012 through mid-May 2013. There are several limitations to the data collected thus far:

- Data have been collected for only a limited period of time (5 months), which does not reflect long-term durability trends.
- The building is still under construction; it is an ongoing renovation project that is projected for completion by December 2014. As a result, most of the building remained at cold interior temperatures through most of the winter, as opposed to typical (heated) interior conditions.
- Many of the joists have not yet received interior insulation, which will be their final operating condition. Other joists have received interior insulation partway through monitoring: this is useful as a before/after comparison.

Interior and exterior temperatures are shown Figure 26; they include both site-collected temperature (T ambient) and airport weather station data (T KLWM) for comparison. Interior conditions (T Logger) roughly track exterior conditions, with some damping due to thermal mass. Semi-permanent construction heating was added to the front of the building on January 17<sup>th</sup>, 2013, resulting in interior temperatures in the 50-75° F (10-24°C) range (T Hallway) at that portion of the building. This temperature was estimated (T Hallway-Estimated) using a “cheek” temperature (side of a joist) at the front of the building. As outside temperatures warmed (early April), the heat was turned off, and the temperatures at the Logger and Hallway converged. The cool spring interior temperatures are due to the sensors being in basement locations (both limited solar gain and coupled to ground temperatures).

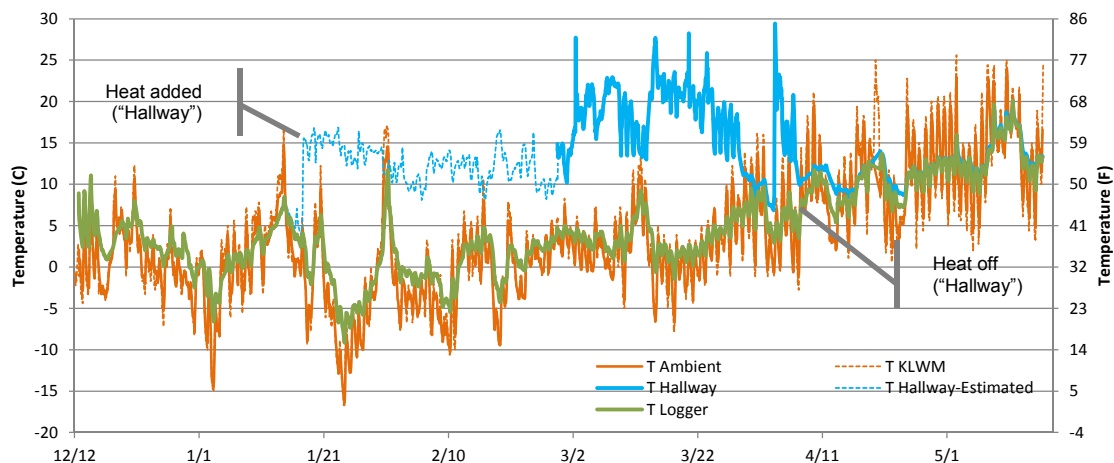


**Figure 26: Interior and exterior temperatures (Lawrence/KLWM airport data for comparison)**

Exterior and interior relative humidity measurements are shown in Figure 27.

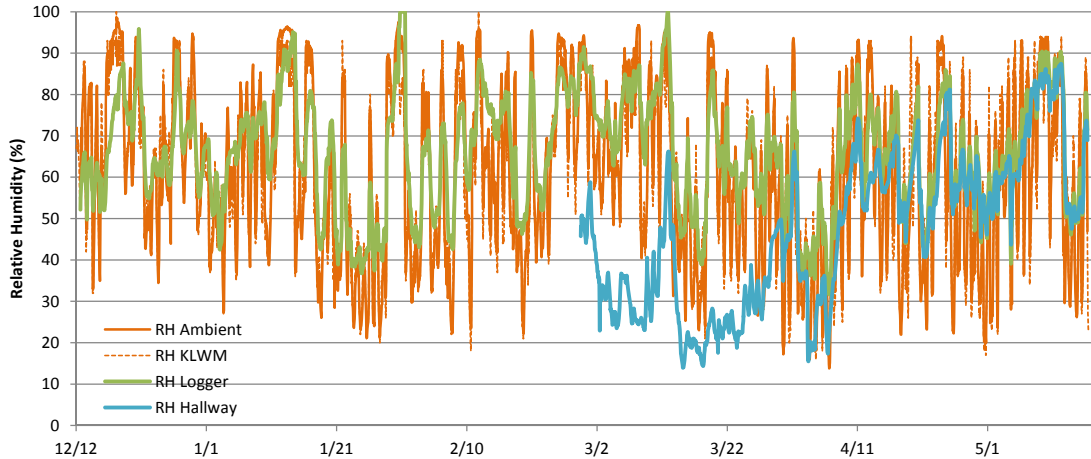


**Figure 27: Interior and exterior relative humidity measurements (KLWM data for comparison)**

However, these data are more useful to plot as dewpoint (absolute moisture content), as shown in Figure 28. Interior dewpoints (DP Logger) track exterior conditions, as would be expected given the high air leakage rate and low occupancy during construction. Interior dewpoint conditions do not correlate to exterior dewpoints exactly; low excursions are damped out. This damping is due to some minimal degree of airtightness, and adsorption/desorption of interior materials. The hallway dewpoint has fewer excursions than the logger location; this is consistent with the fact that the logger location was noticeably air leaky. The low interior wintertime dewpoints are drier than expected occupied wintertime conditions (e.g., 35°F/2°C dewpoint is equivalent to 68°F/20°C/30% RH).

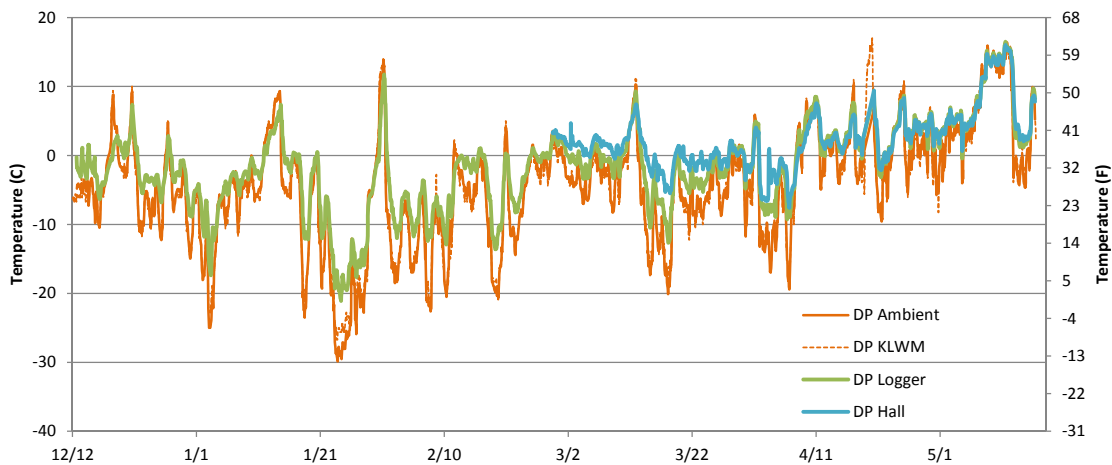


**Figure 28: Interior and exterior dewpoint temperatures (KLWM data for comparison)**

Of course, hygroscopic materials (such as wood joists) react to relative humidity (RH) rather than absolute humidity (as reflected by dewpoint). Given interior humidity measurements typically in the 40-90% range (due to cold temperatures), we would expect wood within the building to operate in the 8-20% moisture content range. Of course, joist pockets are operating at colder conditions than the main space, and are coupled to the potentially wet masonry wall, and are therefore likely to have higher moisture contents.

### Joist Moisture Content Measurements: Unheated Wing Basement

Graphs in this section cover the joist ends on the basement level, in the unheated wing of the building (highlighted in Figure 29).

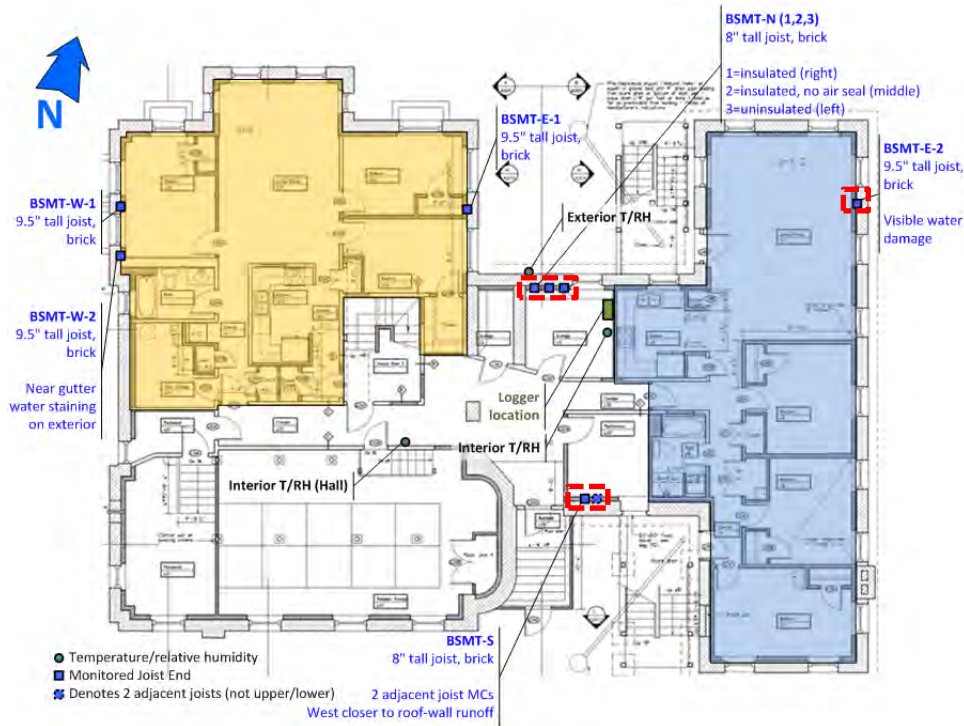


**Figure 29: Basement unheated wing joist end measurements highlighted**

The joist moisture content measurements are graphed showing the moisture content (plotted on the left-hand axis) for the lower and upper joist end locations (“JoistLo and JoistUp”), the “cheek” moisture content measurement (as a comparison point), and the relative humidity measured in the joist pocket (plotted on the right-hand axis). No wood species correction factor is used. Graphs are shown below for the basement level, north-facing joists in Figure 30, Figure 31, and Figure 32.

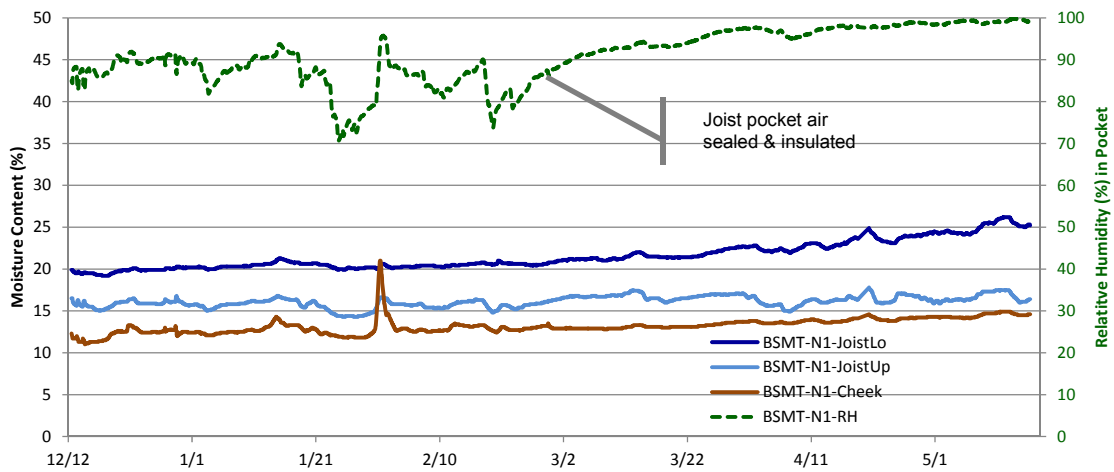


**Figure 30: Basement North 1 (insulated) joist end moisture contents and relative humidity**

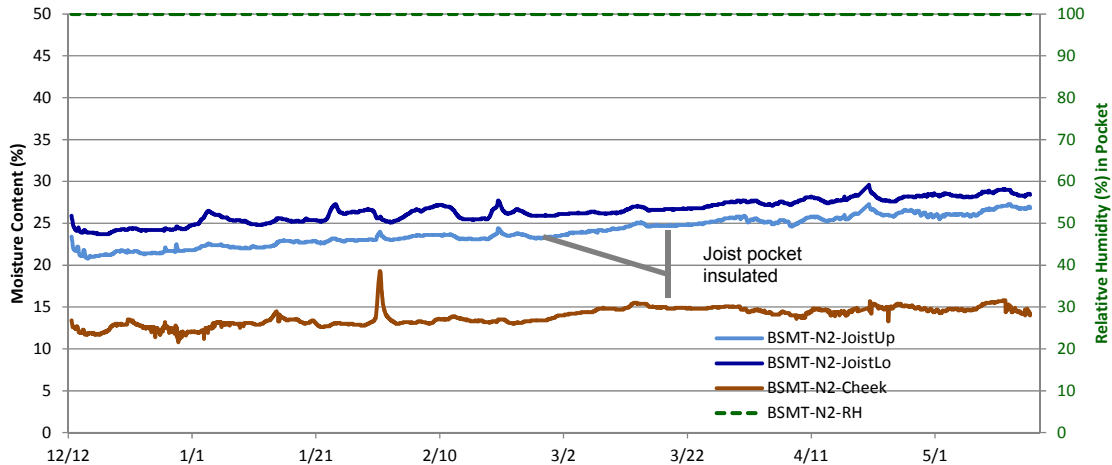


**Figure 31: Basement North 2 (fiberglass) joist end moisture contents and relative humidity**

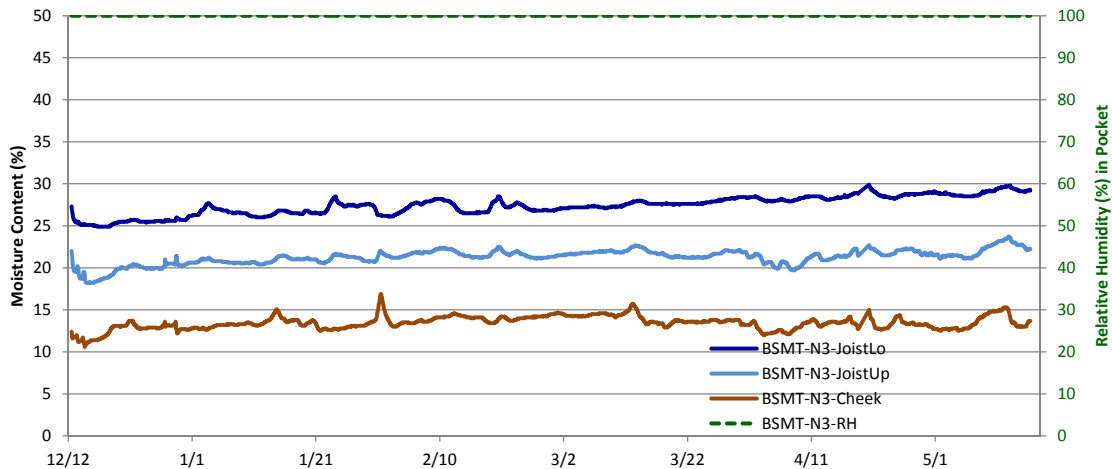


**Figure 32: Basement North 3 (uninsulated) joist end moisture contents and relative humidity**

During this period, this wing was running at unheated conditions (as per the “T Logger” sensor).

The joist pocket relative humidity measurements showed high levels, of either constant 100% (BSMT-N2 and BSMT-N3), or in the 80-100% range (BSMT-N1). The reason for the RH difference between BSMT-N1 vs. BSMT-N2/N3 was not evident from visual or infrared observations. Temperature measurements showed that the largest differences between joist ends were 1°F/0.5°C, and visual inspection of the T/RH sensor installation did not show any significant installation differences between N1, N2, and N3.

Moisture content measurements consistently showed that the lower joist end (JoistLo) was wetter than the upper joist end (JoistHi). This can be attributed to direct contact with the masonry pocket, gravity drainage of bulk water, greater drying at the top of the beam/deeper embedment at the bottom of the beam, and/or more of an air pocket at the top of the beam. The cheek measurement was dryer than the joist end measurements in all cases. BSMT-N1 has moisture contents lower (drier) than BSMT-N2 and BSMT-N3, which is consistent with the relative humidity measurements.

The joist end moisture contents are higher than typical levels recommended for durability: lower joist ends are in the 20-30% range; upper joist ends 15-27%, and joist cheeks 10-15%. As discussed previously, this reflects unheated or “mothballed” building conditions. However, no noticeable damage to the beam ends was evident during sensor installation.

The insulation and air sealing of the joist pocket (BSMT-N1) and installation of fiberglass insulation (BSMT-N2) were completed on February 27, 2013. The relative humidity in the joist pocket of the foamed and air sealed joist (BSMT-N1) slowly rises after air sealing, approaching 100% RH levels. The pocket wood moisture contents in a similar manner. Note that outdoor temperatures are rising during this period as well; measurements reflect both changes. The fiberglass insulated joist (BSMT-N2) also shows a slight rise in joist end moisture contents after insulation.

Measurements from the east-facing joist from the rear of the building are shown in Figure 33; moisture contents are higher here than on the north side (~35-40% lower; ~30% upper). This is consistent with the evidence of previous water leakage (see Figure 11). In addition, this orientation has the highest driving rain exposure (see Figure 3). There was a loss in data from March 7 to 14, 2013 due to damage to the extension wire. Moisture content, temperature, and relative humidity measurements were all affected at that time.

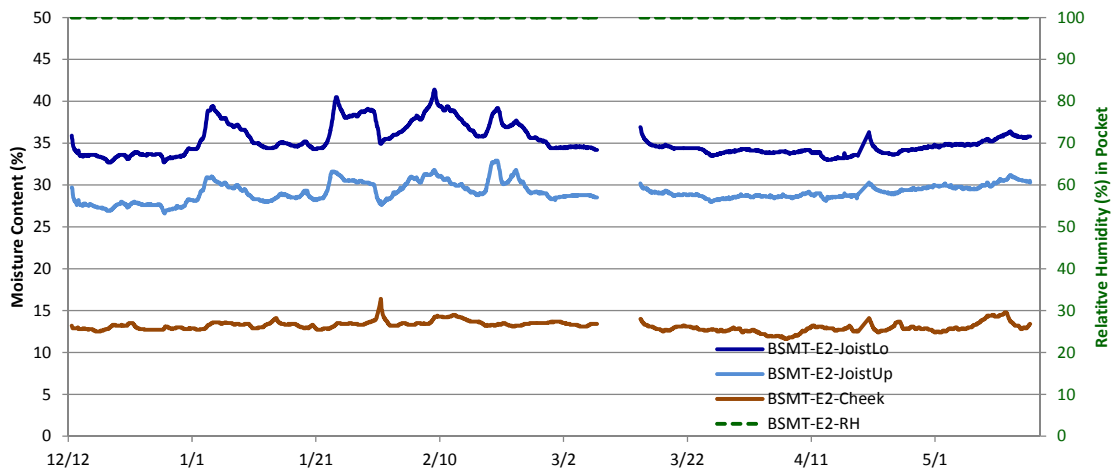


**Figure 33: Basement East 2 joist end moisture contents and relative humidity**

The south-facing basement joist is plotted in Figure 34; moisture contents are substantially lower (~10%) than the north- and east-facing basement joists, and the relative humidity is markedly lower (centered on 80% RH). There is little difference between the joist and cheek measurements; the wood may be at equilibrium with interior conditions at all measurement points. The joist pocket was air sealed and insulated sometime in late April/early May; the rise in humidity and moisture content might be associated with this change.

Note that the BSMT-S joist end measurements are a left/right pairing, not an upper/lower pairing.

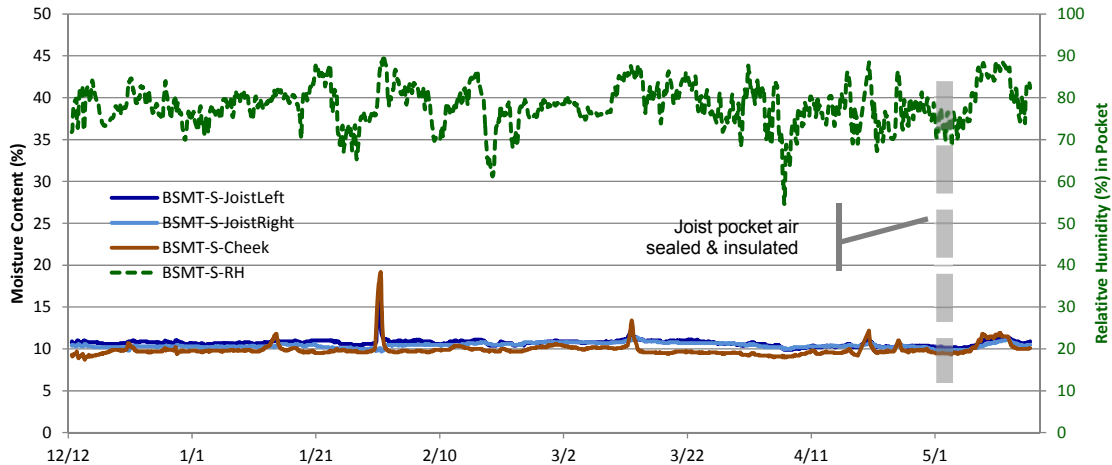


**Figure 34: Basement South joist end moisture contents and relative humidity**

The basement south joist shares interior conditions with the north- and east-facing joists; the difference is likely the effect of solar heating. The joist pocket temperatures for north facing (BSMT-N1, -N2, and -N3) and south-facing (BSMT-S) joists are compared in Figure 35; the south side is slightly but consistently warmer. Joist end temperatures converge as outdoor temperatures rise. The low moisture contents may be due to this solar heating, as well as low driving rain exposure.

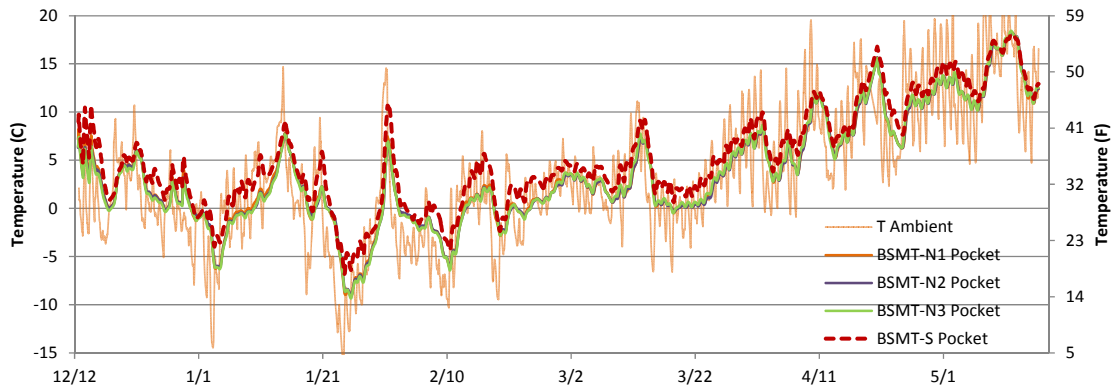


**Figure 35: Basement North and South joist pocket temperature comparison**

**Joist Moisture Content Measurements: Unheated Wing First Floor**

Graphs in this section cover the joist ends on the first floor, at the rear portion of the building (highlighted in Figure 36). During this period, this wing was running at unheated conditions. The joist ends on this floor are primarily installed in hollow clay block backup wall, although some solid brick is mixed in to the wall assembly.

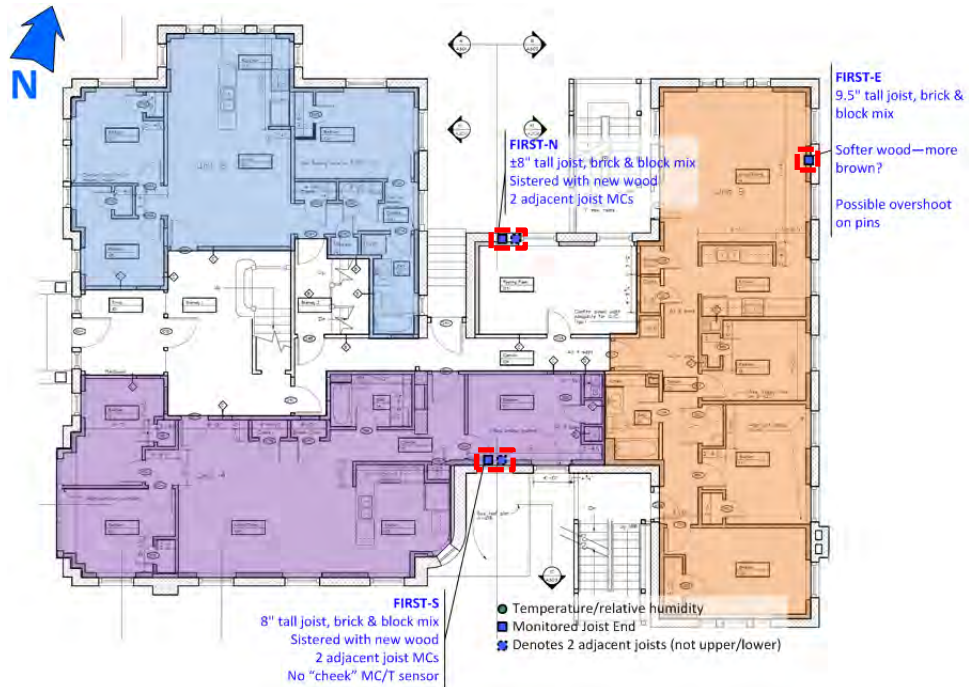


**Figure 36: First floor unheated wing joist end measurements highlighted**

The north-facing joists (left/right) measurements are shown in Figure 37; the left-facing joist (FIRST-N-JoistLeft) is cropped from the plot, as it has measurements in the 48-60% range. This is far higher than any other measurements in the building; the reason for this anomaly has not been positively determined. However, it is likely that the pins are somehow short circuited through the masonry or grout, given the measurement of a constant 14-15 kΩ (the apparent moisture content changes are due to temperature correction). The beam pocket relative humidity remains at 100% throughout these measurements. Similar to previous measurements, the cheek moisture content is lower (drier) than the joist end MC. The joist pocket moisture content shows a slight but discernible rise in moisture content (25 to 30%) over the course of monitoring.

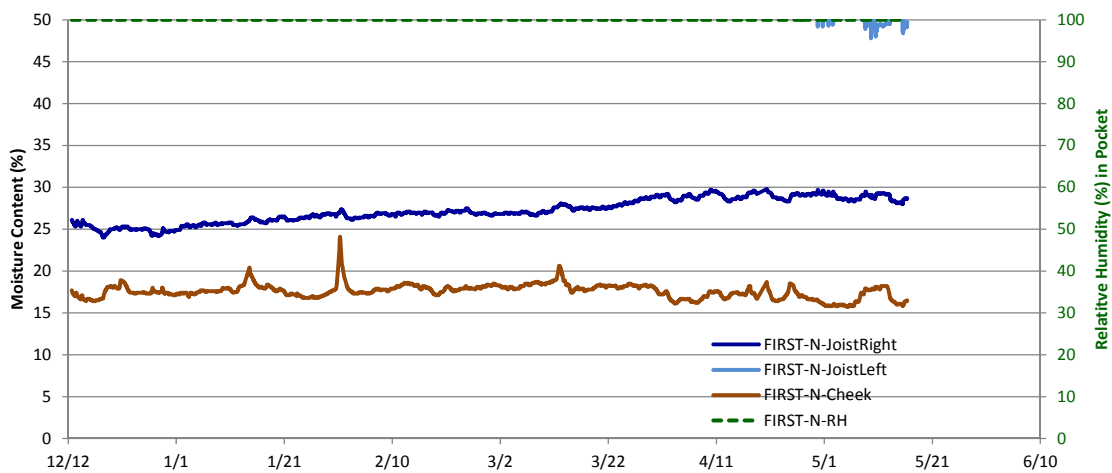


**Figure 37: First North joist end moisture contents and relative humidity**

The first floor east (FIRST-E) measurements show low moisture contents of roughly 10-13%; it should be noted that this joist was the softer brown wood noted earlier. However, the measured pocket relative humidities (80-90% RH) are consistent with lower moisture content measurements. Cheek and joist end moisture contents were identical in winter, but the cheek is noticeably drier in the spring, as outdoor temperatures rose. These low moisture contents occur despite a high driving rain exposure on this orientation.

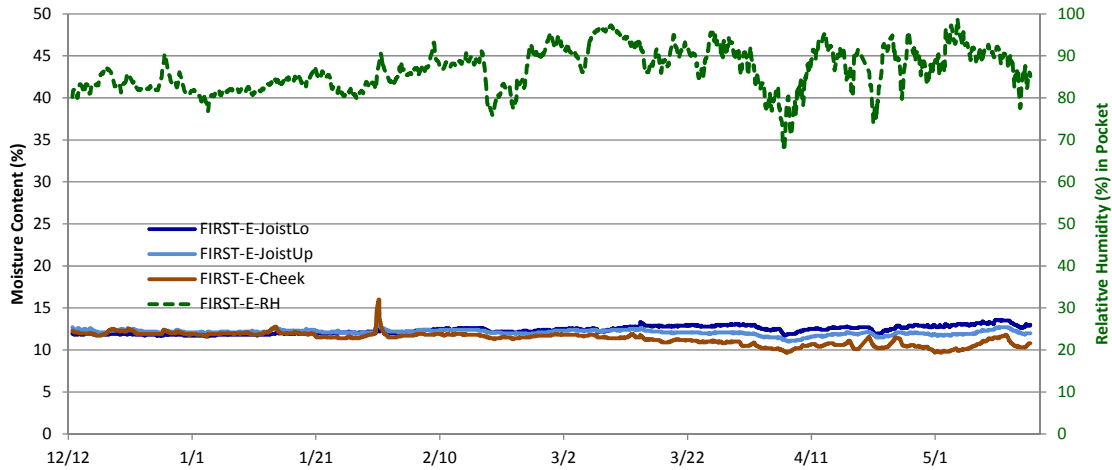


**Figure 38: First East joist end moisture contents and relative humidity**

The south-facing joist moisture contents are also low (8-11% MC), with consistent RH measurements (50-80% RH). Note that there is no joist cheek measurement at this joist.

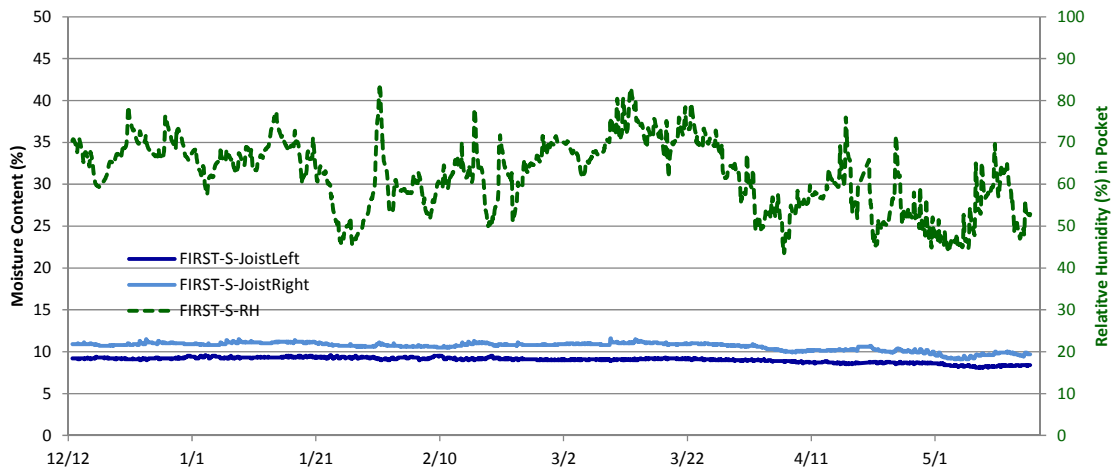


**Figure 39: First South joist end moisture contents and relative humidity**

***Joist Moisture Content Measurements: Heated Wing Basement***

Graphs in this section cover the joist ends on the basement level, in the section that was running at unheated conditions until January 17<sup>th</sup> 2013, when semi-permanent construction heat raised interior temperature to the 50-75°F (10-24°C) range (as per the T Hallway sensor). The locations of these measurements are highlighted in Figure 40.

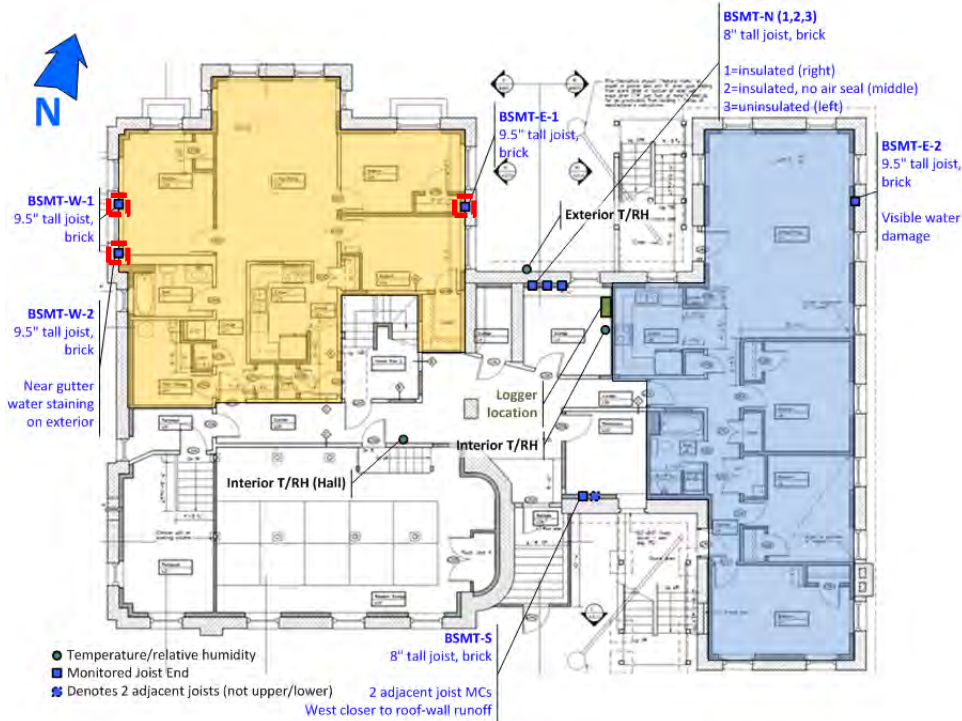


**Figure 40: Basement heated wing joist end measurements highlighted**

The east-facing joist (BSMT-E1) shows similar patterns to previous measurements, in terms of the relationship between the upper, lower, and cheek moisture content measurements. However, the lower joist moisture content measurement is noticeably wetter (40-50% MC) than other measurements. This is much higher than would be expected for good durability. Relative humidity measurements are consistent with high MCs. In terms of exposure, even though this joist faces east, this location is blocked from solar gain by the adjacent wing (see Figure 40); it also has high driving rain exposure (Figure 3).

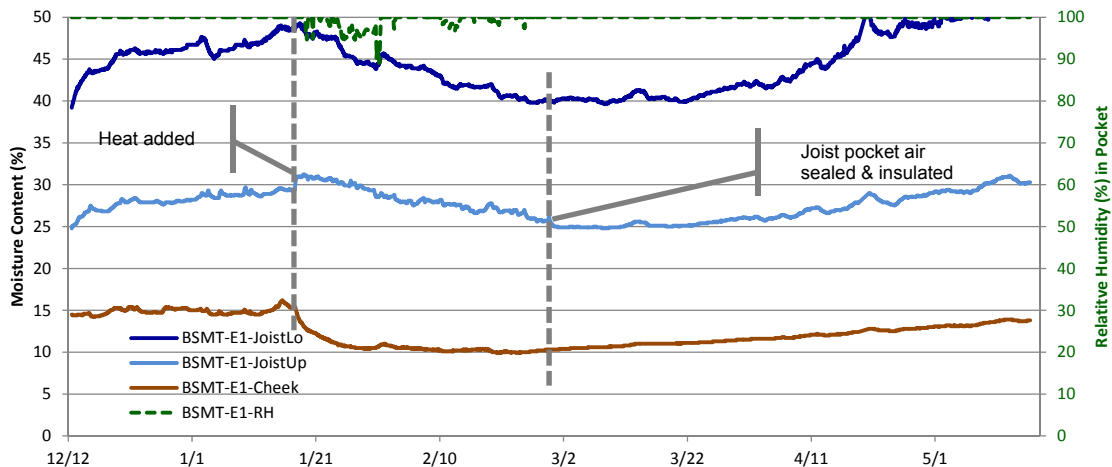


**Figure 41: Basement East-1 joist end moisture contents and relative humidity**

After the addition of interior heat (January 17<sup>th</sup>), moisture contents begin to fall, especially at the joist cheek (which has the greatest exposure, and the most drying available). In addition, the relative humidity in the joist pocket begins to move off of 100%.

However, air sealing/insulating with spray foam at the joist pocket (February 27<sup>th</sup>) caused a marked change: the relative humidity rose back to a constant 100%, and the moisture contents began to rise towards previous levels. In addition, the joist end moisture contents show less day-to-day variability. The “cheek” moisture content also rises: it is “buried” within the spray foam insulation, so it is isolated from interior conditions.

The west-facing joists start at drier conditions than the east-facing joist (15-30% MC), and show marked drying after the addition of interior heat. The effect of interior heating is also clearly shown in the relative humidity measurements, which drop from 90-100% to 60-90%. Note that the intermittent cheek MC signal (between “Heat added” and insulation/air sealing) is due to the wood being at the lower limit of measurement range.

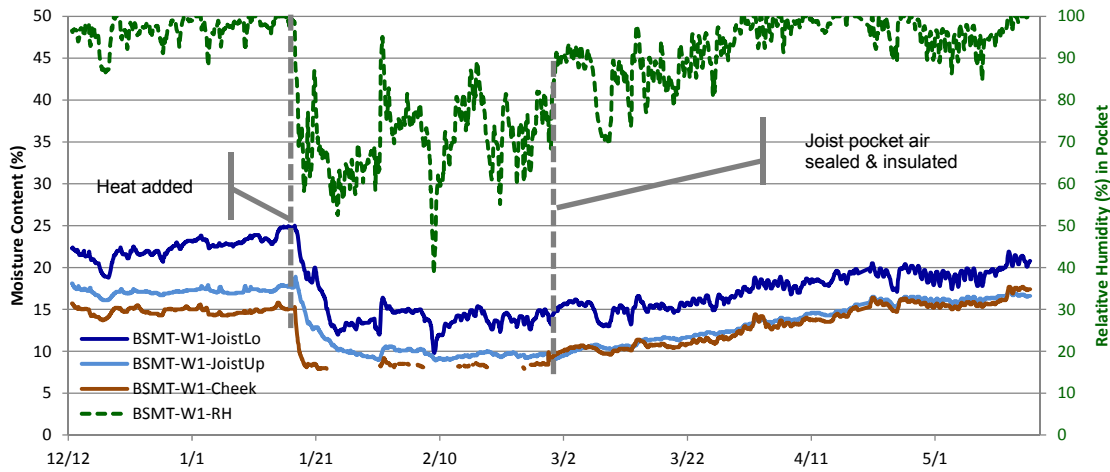


**Figure 42: Basement West-1 joist end moisture contents and relative humidity**

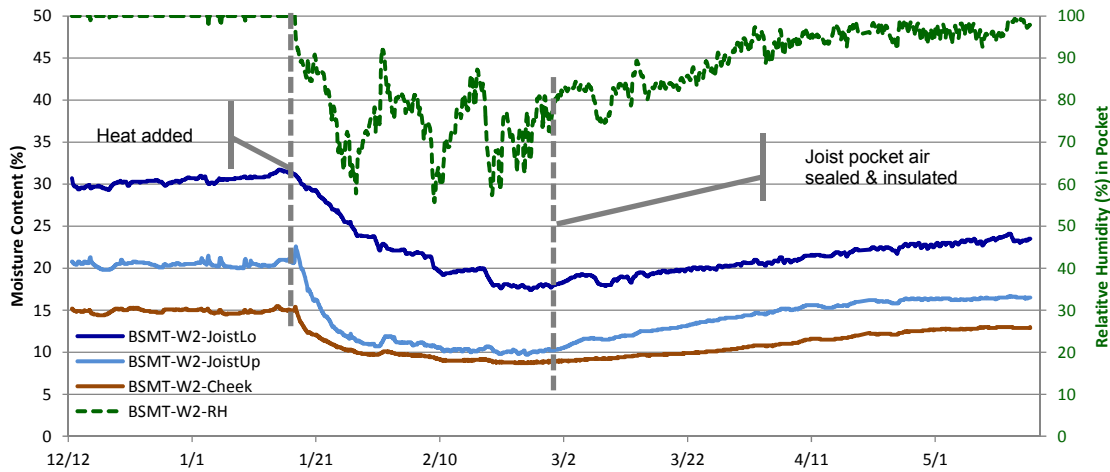


**Figure 43: Basement West-2 joist end moisture contents and relative humidity**

The effect of air sealing the joist pockets (February 27<sup>th</sup>) is similar to the east-facing joist: relative humidity and moisture measurements start creeping upwards.

The RH and MC differences between east- and west-facing joists are consistent with temperature differences within the pocket, as shown in Figure 44. The west-facing joist pockets have a much larger increase in temperature after the addition of heat, compared to the east-facing joist. The space heater for the front of the building is closer to the west-facing joists (front) than the east-facing joist. The temperature difference continues after heat is shut off: the east-facing joist is shaded from solar gain by the adjacent portions of the building (see Figure 40).

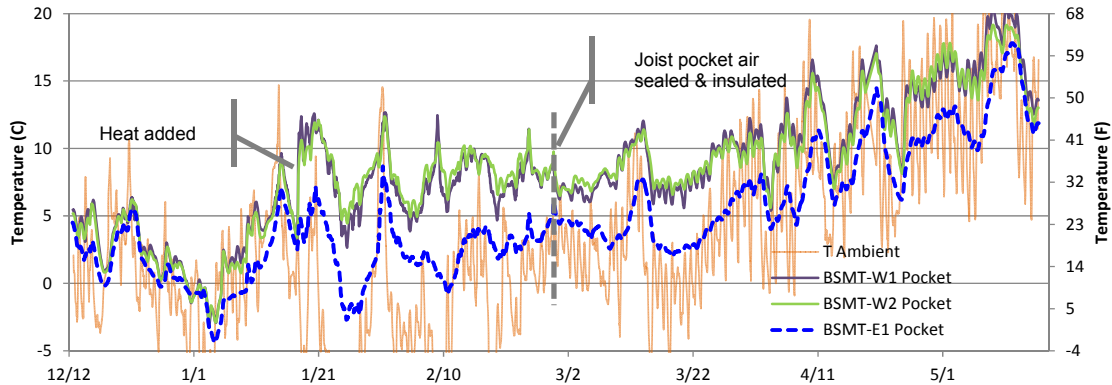


**Figure 44: Basement West & East joist end temperature comparison**

### Conclusions and Further Work

Specific answers to the research questions from the test plan can be found in the final section of the report, “6. Research Question Answers and Further Work.”

### Analysis and Interpretation

One key conclusion is on the field monitoring methodology for monitoring joist end moisture conditions. The extended wood moisture content pins (installed at an oblique angle into the embedded wood member) appear to be returning valid and relevant data, and match the relative humidity data being collected within the joist “pocket.” This installation method has the advantage of not disturbing or demolishing the masonry pocket surrounding the joist end (as done by Maurenbrecher et al. 1998). This demolition changes the existing conditions of the pocket, and introduces construction moisture (new mortar) into the system.

Elevated (wetter) joist end moisture contents were accompanied by high relative humidity levels in the joist pocket. Typical high measurements were 90-100% RH, with many joist pockets at a constant 100% RH. Lower (drier) joist end moisture contents were accompanied by lower RH levels.

There was a repeated pattern of joist end moisture content measurements at the upper and lower portions of the pocket. The lower joist end was consistently wetter than the upper joist end, which can be attributed to contact with the masonry pocket, gravity drainage of bulk water to the bottom of the pocket, greater drying at the top of the beam/deeper embedment at the bottom of the beam, and/or more of an air pocket at the top of the beam. The cheek measurements were

dryer than the joist end measurements in almost all cases, due to greater hygrothermal connection to interior space than the masonry pocket.

Some interesting conclusions can be gleaned from the first 5 months of collected data. The building was previously in a “mothballed” or completely unheated condition (boiler removed for scrap) since at least summer 2011, if not earlier. Therefore, initial conditions reflect the behavior of wood joists in an unheated building, in its second winter without heat. This is not an atypical condition for existing mass masonry buildings being renovated and rehabilitated into housing units.

Many of the joists show high moisture contents, with some continuously in the 20-30% MC range, and one outlier even higher (40%+). Although this is a level which causes concern for mold growth and wood decay, no evidence was found of moisture-related damage to the embedded joist ends during sensor installation (which included drilling into the joist ends). These joists, of course, are old-growth wood consistent with circa 1906/1930 construction, which are more resistant to moisture-induced damage.

Orientation was an important factor in resulting moisture contents. The highest moisture contents were found on north side, and the east-facing sun-sheltered location. Lower moisture contents were found on other orientations, especially on the south side of the building, which receives the greatest solar heating. The south and first floor east measurements were within the safe range for wood moisture damage, even in unheated portions of the building (10-13% MC range). Based on the measured temperatures, the consistent elevated temperature appears to play a factor in these lower moisture contents. The driving rain exposure may also play a role; the north and east elevations have the highest exposures. However, low moisture content seen at the first floor east joist, which is not consistent with high driving rain exposure.

There is weak evidence to suggest that joists embedded in hollow clay block (as opposed to brick) might have greater drying, but the sample size is too small to draw any conclusions.

Interior heating was added in mid-January 2013 at a portion of the building, which was reflected by measurements in three joist end sensors. It showed that interior heating—even with the presence of interior insulation—can be significant in drying joist ends. Before the addition of heat, the joist end moisture contents were in the 20-30% MC range. After the addition of heat, moisture contents fell to a safer range (10-20%). This pattern correlated exactly with the addition of heat, and is not a function of warmer outdoor temperatures. The degree of drying was related to the temperature in the joist end pocket: the joist ends closer to the heating unit dried faster than one away from the heater.

Several joist pockets were insulated and air sealed in late February, 2013 (in both heated and unheated spaces). They showed a consistent pattern: relative humidity steadily rose to high levels (to 90-100%), and joist end moisture contents rose. This shows the effect of coupling the joist end to the masonry pocket, which likely has stored water in the brick, and is therefore at wetter conditions than the interior space. At first, this might seem to be a reason to leave the masonry pocket open to the interior, to “allow drying.” However, typical interior humidity levels are high enough that there are wintertime condensation risks in the cold masonry pockets,

if this air leakage occurs. Winter of 2012-2013 may demonstrate the effects of air sealing vs. allowing air transport (comparing BSMT-N1 and -N2).

In addition, cheek moisture content measurements typically rose after insulation/air sealing. The interior insulation typically enveloped the cheek measurement location in spray foam.

There is no evidence so far of joist end moisture content response to rain events; however, based on previous work (Ueno 2008), wood moisture contents often have a relative slow response, especially when adsorbing/gaining moisture. Rain impacts are more likely to appear in the data as seasonal effects, rather than in response to individual wind-driven rain events.

### ***Further Work***

The intent is to continue data collection at this monitoring installation over time, to provide insight into the long-term durability of the interior insulation retrofit. For instance, it is expected that during warmer summertime weather, the moisture content in the joist end will fall (wood will dry). On the other hand, summertime often has high levels of precipitation; the response (if any) of the joist end moisture content to wind-driven rain events will be examined.

As noted above, the renovation's projected completion date is as late as December 2014, which leaves a substantial period before all of the units are completed and occupied. However, some of the units are likely to be completed before others. Overall, the longer that data can be collected (within limits), the greater the value of these results.

An additional suggested explanation for the higher moisture contents at the "lower" joist location is migration of salts from the masonry into the wood, which would increase apparent moisture content due to electrical conductivity changes. If additional work can be budgeted, spatial differences in salt content can be examined by analyzing drilled wood shavings.

A key observation planned for the long-term monitoring is determining whether the seasonal moisture cycling results in a net increase in moisture levels over time, or "ratcheting." This behavior would tend to indicate long-term durability risks, especially if moisture levels are rising to levels consistent with mold growth and rot for wood members.

If certain monitored locations are observed to have consistently high moisture levels, the building owners will be informed, and intrusive disassembly may be performed to determine the source of the moisture issues. The three joists with different interior retrofit strategies (XPS insulation with air barrier, fiberglass insulation without air barrier, and uninsulated) are located in a common basement storage room, so retrofitting poorly performing options will be simpler than a retrofit in an occupied unit.

### 3 Use of General Masonry Characteristics and Basic Materials Testing

Frost dilatometry (measurement of masonry critical degree of saturation/ $S_{crit}$ ) is used to assess freeze-thaw risks to masonry buildings retrofitted with interior thermal insulation. However, the associated testing and simulation activities add project cost and time requirements. Some practitioners have questioned whether frost dilatometry testing is required in every case, and whether generalizations could be made based on more easily obtained properties. This work in this section included an analysis of the database of 24 previous projects, to determine whether generalizations could be made.

#### Introduction

The frost dilatometry approach described in this document is used to assess freeze thaw risk to masonry buildings retrofitted with interior thermal insulation. The test method is covered in further detail by Mensinga et al. (2010). The overall approach to risk assessment begins with a field inspection (common to most building retrofits), but adds material property testing and hygrothermal analysis. The testing and simulation activities add project cost and time requirements, so developers are often reluctant to pursue these investigations, opting to leave the building uninsulated or to 'insulate blind' using generic and potentially inappropriate techniques. Some practitioners have questioned whether frost dilatometry testing is required in every case, and whether generalizations could be made based on more easily obtained properties, such as manufacturer, manufacturing method (pressed vs. extruded brick), vintage, density, porosity, etc. Having these types of generalizations would simplify risk assessments for interior insulation, potentially enabling more projects to insulate.

A related effort was made by an Illinois State Geology Survey study by Hughes and Bargh (1982). Their goal was to establish connections between brick type, building location and 'degree of weathering' or material deterioration. Ultimately, the association of brick type and degree of weathering does not appear in the report. The difficulty with achieving this goal is perhaps addressed in their statement:

*The study of brick weathering is much more complicated than the study of limestone weathering. The composition and firing history of the bricks, the composition and production history of the mortar, the quality of construction, the location of the structure geographically, the details of design of the particular structure all lead to a multitude of variables to be isolated and examined in the study of masonry weathering. (Hughes and Bargh 1982)*

Laefer et. al. (2004) encountered similar challenges: they describe a lack of uniformity caused by the molding and firing methods, as well as the composition of the brick raw materials. Their study focused on strength properties, but also included absorption measurements with 242 to 300% high/low differences.

Hence, finding a link between identified brick types and the extent of weathering proves quite difficult. Past studies attempted to generalize masonry performance to avoid testing. In this section we investigate opportunities to categorize masonry materials, in an effort to reduce the scope of testing. The investigation is based on analysis of our current material property testing

results database from previous projects. These insights are framed around the various material properties used as input data for hygrothermal simulation and post processing. At the end of the section, the findings are used to illustrate the challenges with more general interpretation of visual characteristics, and potentially reducing material testing requirements. The presentation of the data is also intended to provide building scientists with a significant dataset for brick, terra cotta, and various stones used on North American building walls assemblies.

### Existing Material Property Data

Within our assessments, a number of material properties are determined through laboratory testing and then used in hygrothermal modeling (typically WUFI/Wärme- Und Feuchttransport Instationär, Künzle 2002). A Material Data dialog box from WUFI is shown in , which includes the various heat and moisture transport and storage properties described below.

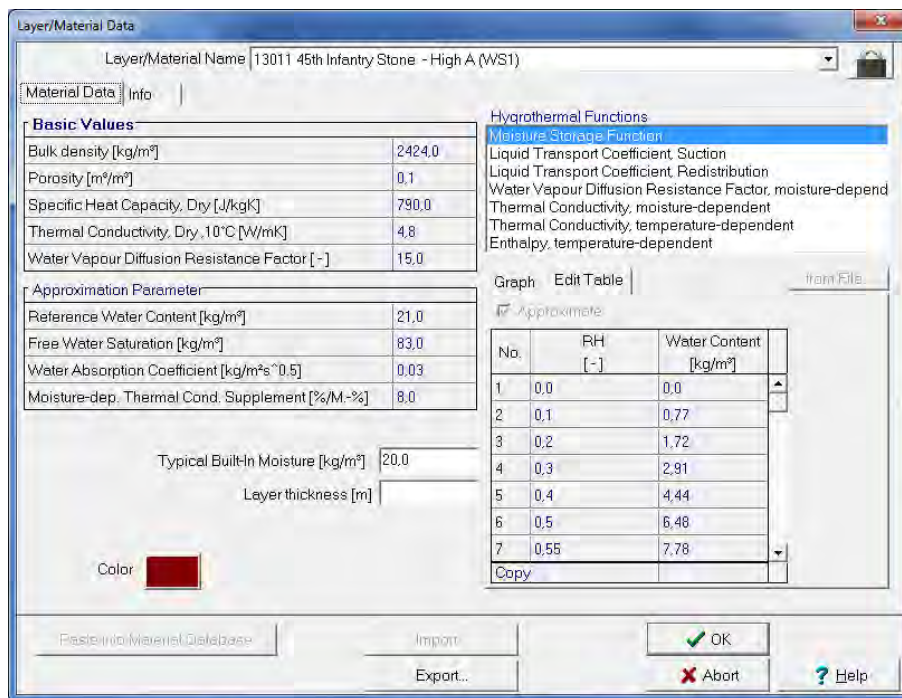


**Figure 45: WUFI Layer/Material data dialog box**

- Bulk (dry) density, porosity (vacuum saturation), free water saturation, and water absorption coefficient are all measured in our laboratory testing and will be explored in this section.
- Reference water content ( $W_{ref}$ ) or water content at 80% RH, has only recently been added to the testing regimen, and the database is too small to be considered in this study.
- Specific Heat Capacity and Moisture-Dependent Thermal Conductivity Supplement are estimated for different materials based on values published in ASHRAE *Handbook of Fundamentals* (2009).
- Thermal Conductivity is estimated by linear interpolation based on density and values also found in ASHRAE (2009).

- Water Vapor Diffusion Resistance Factor is analyzed using high and low values included in WUFI’s material database, and is not typically derived from testing due to long testing time requirements.

A full explanation of these material properties is beyond the scope of this document; further information can be found in Künzel (1995), and Straube and Burnett (2005).

These input parameters are used to predict the conditions within masonry units during freeze-thaw events for the climate and exposure of the wall of interest. The predicted peak moisture contents are then compared to the critical freeze-thaw moisture content (Scrit) of the masonry layers in post-processing. Incidents when moisture content exceeds Scrit can then be used to assess the risk of freeze-thaw damage due to various retrofit strategies.

The input material properties could be drawn from the various sample masonry materials included in the WUFI database and analyzed through sensitivity analysis. This approach has two major limitations; 1) there is limited Scrit data available in literature, and; 2) this analysis would result in a large range of outcomes—from low to high risk of deterioration—providing limited insight. Hence, material data representative of the actual wall system under investigation is necessary.

### Sample Dataset

The dataset is drawn from results of 24 previous projects involving testing at some level. Each project listing shows the state or province (as an abbreviation), brick manufacturing type (pressed or molded), and the masonry type.

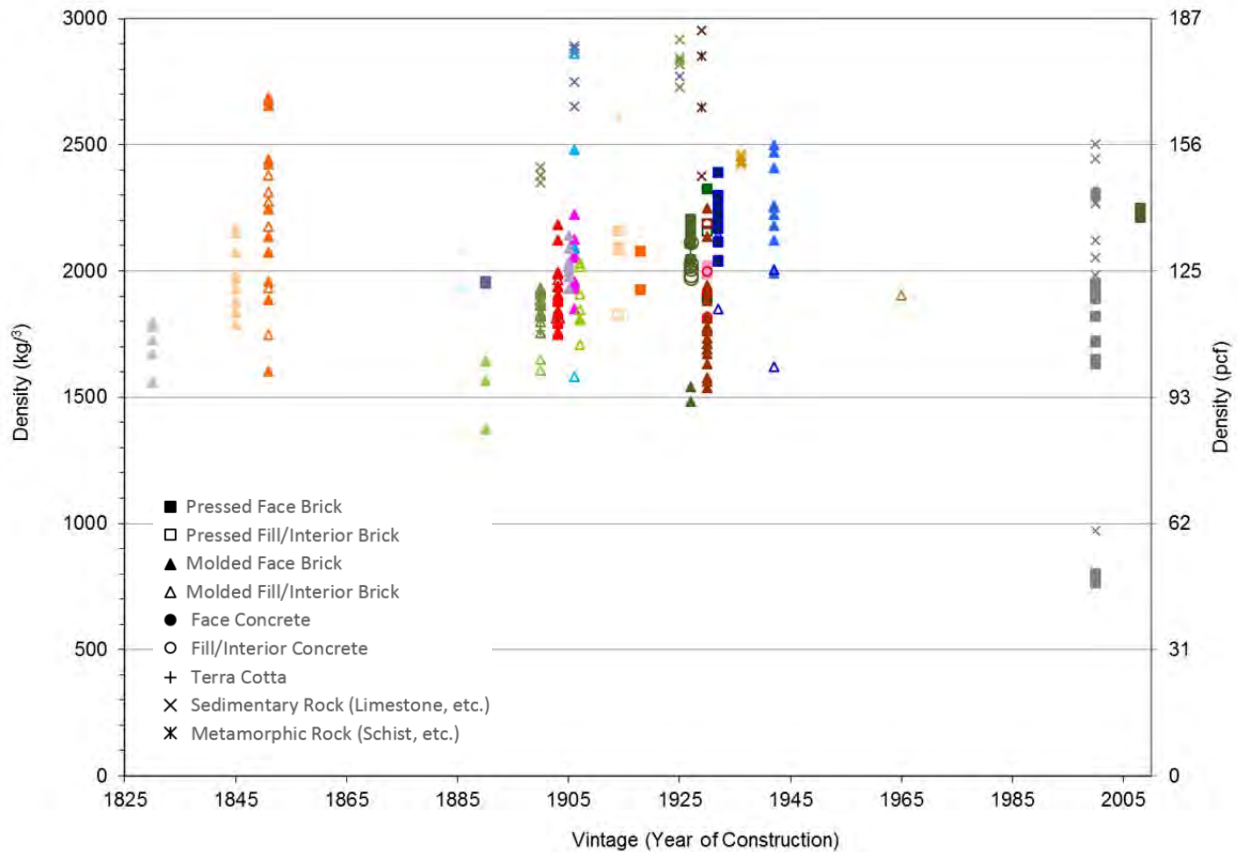


Figure 46: Sample set legend

Most of the plots are given with vintage as the horizontal axis, providing a separation between projects and even building wings within projects. Some projects contain several types of masonry materials. The legend provided in Figure 46 illustrates the marker coding, and shows the geographic range of collected samples.

### Dry Density

Dry density test results for brick, stone, and terra cotta samples are plotted against vintage (estimated from the building's year of construction) in Figure 47. No clear correlation between vintage and dry density is apparent for tested bricks; the majority of these samples are pre-1940's vintage. Furthermore, no clear correlation between geographic locations (represented by varying colors) is apparent.



**Figure 47: Dry density vs. Vintage**

### Porosity

Porosity (measured by vacuum saturation) is generally greater for older bricks as shown in Figure 48. It is noted that there are fewer projects included within this plot than in Figure 47, as only more recent testing included vacuum saturation. Inner and fill bricks tend to have higher porosity than face bricks. Molded bricks tend to have a higher porosity than extruded bricks. Similar to dry density, there is as much as 50% variation in porosity for some bricks from the same building, which are presumably of the same vintage, manufacturer, etc.

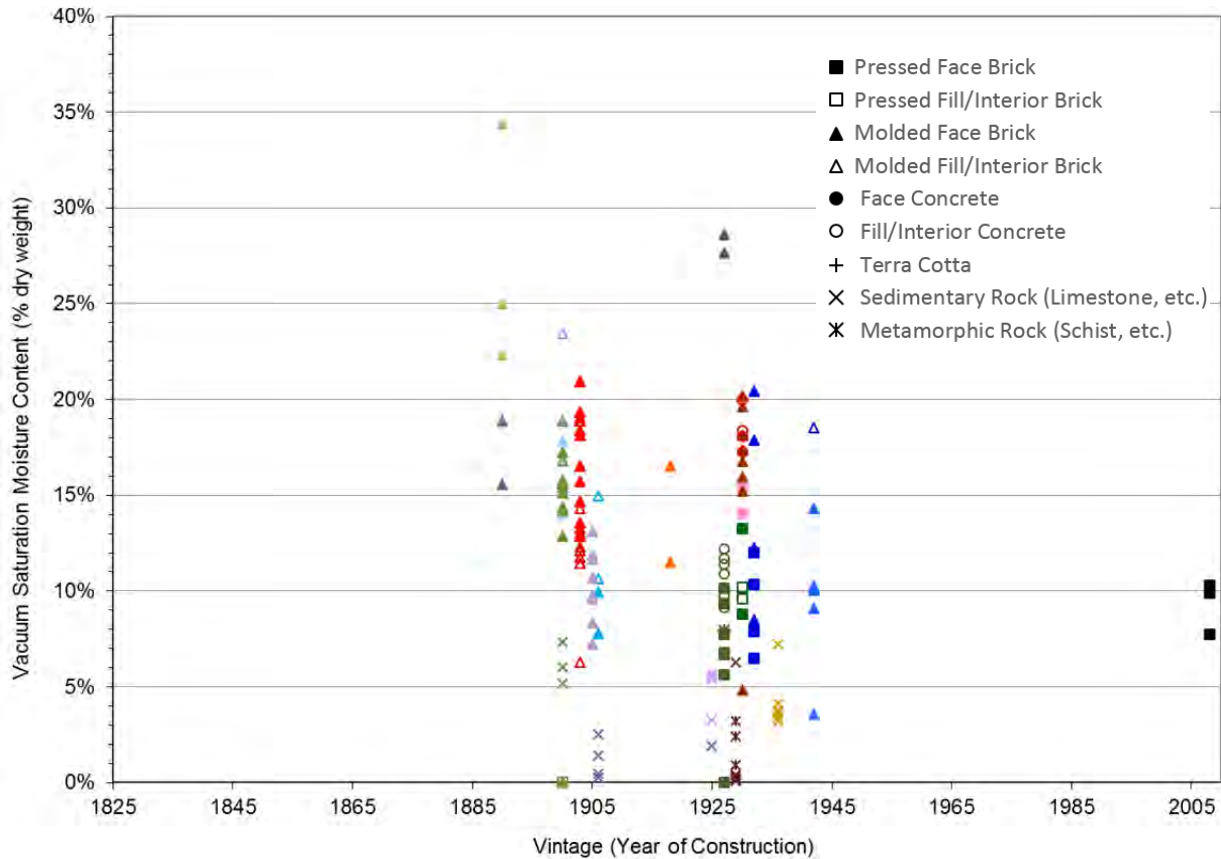


**Figure 48: Vacuum saturation vs. Vintage**

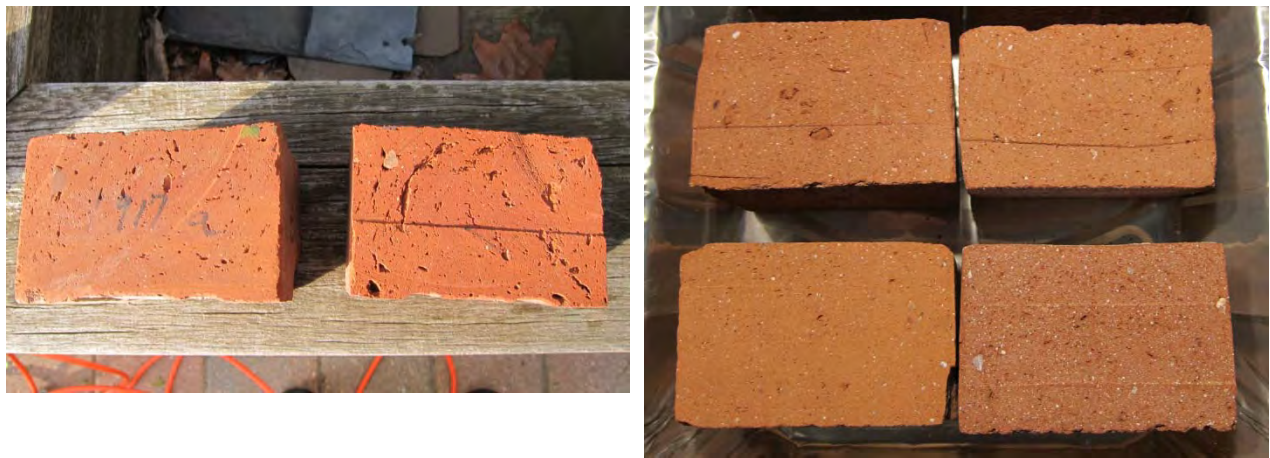


**Figure 49: Highly porous c. 1917 (left) and less porous c. 1940 (right) brick samples**

### Water Uptake Coefficient

Water Uptake Coefficient (or A-value) is generally greater for older bricks, as shown in Figure 50. No clear correlation with inner and fill bricks relative to face bricks is apparent. Molded bricks tend to have higher uptake coefficients than extruded (pressed) bricks, although there is considerable overlap. Note that Figure 50 is a logarithmic plot, reflecting the large range of A-values found in brick samples. Bricks from the same building (which are presumably of the same vintage, manufacturer, etc.) have A-values varying by 2 orders of magnitude or more.

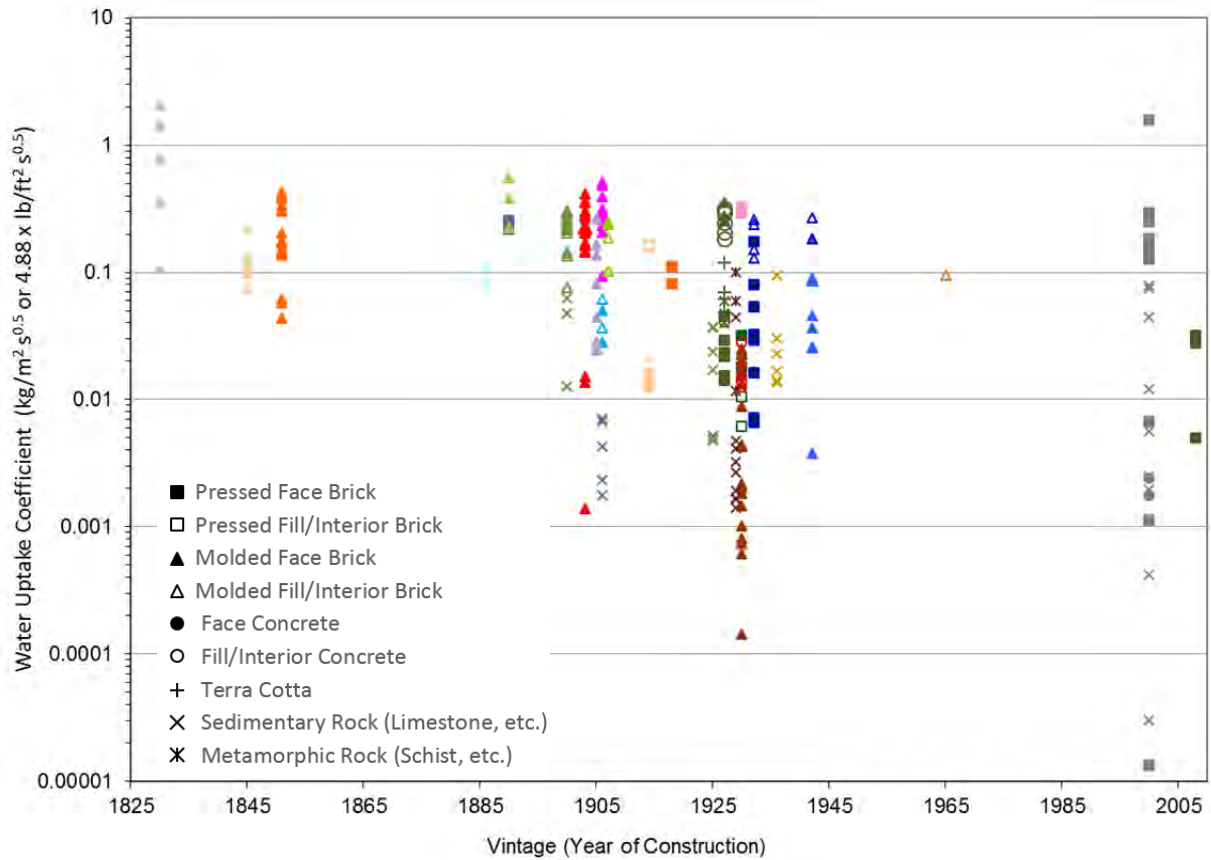


Figure 50: Water uptake coefficient vs. Vintage



Figure 51: Brick water uptake coefficient (A-value) testing

### Free Water Saturation

Free water saturation (or capillary saturation) is a measure of how much water the material absorbs under normal pressure (without additional pressure forcing water into the pores). The test method is similar to a water uptake test (Figure 51), except it is done in a closed container to limit evaporation. The sample will reach a maximum weight/water content, which is equal to the free water saturation.

In contrast, a 24 hour cold soak test (ASTM Standard C 67, ASTM 2009) involves submerging a sample in room temperature (60 to 86°F/15.5 to 30°C) water. The cold soak test is expected to have a slightly higher value, due to hydrostatic head pressure forcing water into the sample pores.

Free water saturation measurements were plotted relative to vintage in Figure 50. In this graph, the value for 24 hour cold soak was used where free water saturation was not available.

No clear correlation between free water saturation and vintage was found, as shown in Figure 52. The stone samples were generally found to have lower free water saturation values than bricks. Within the brick samples, no correlations are obvious.

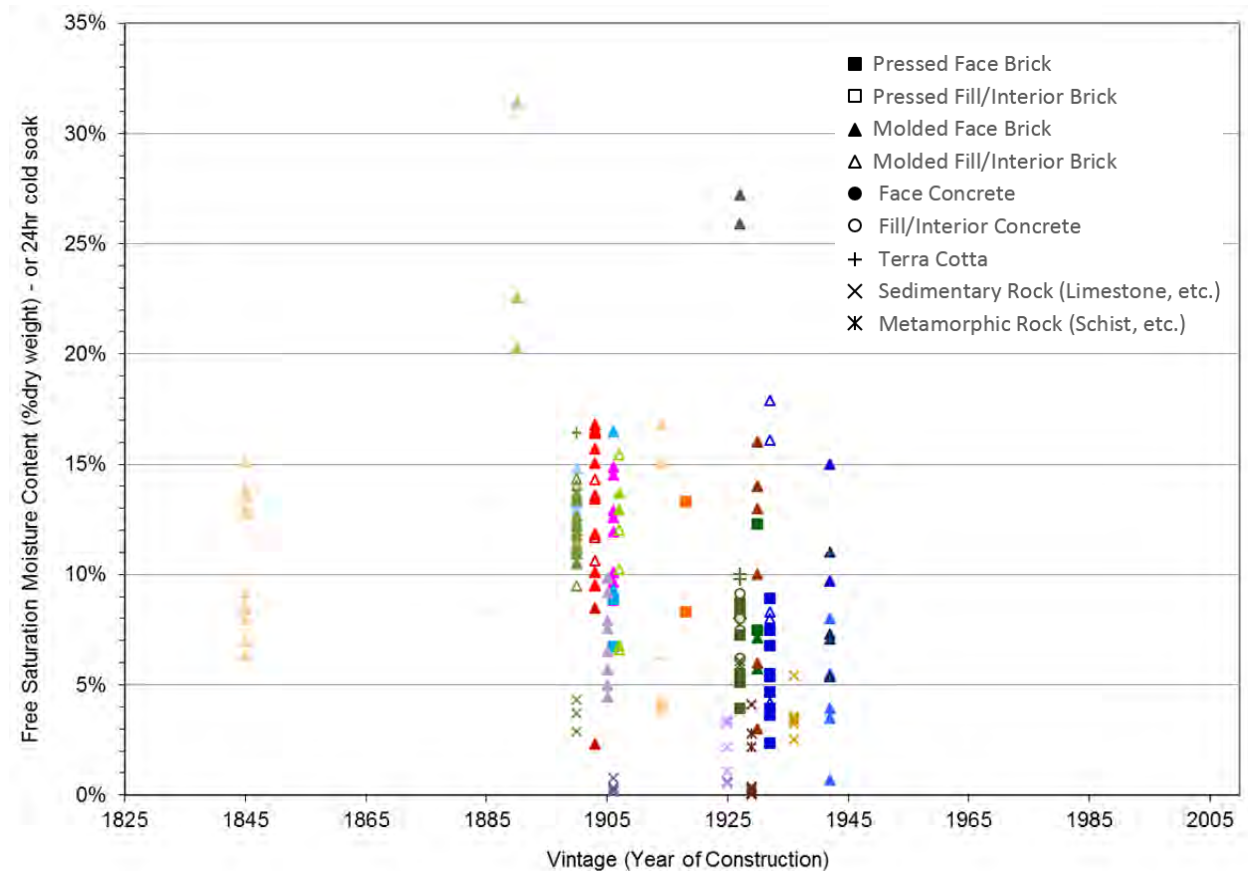


Figure 52: Free water saturation vs. Vintage



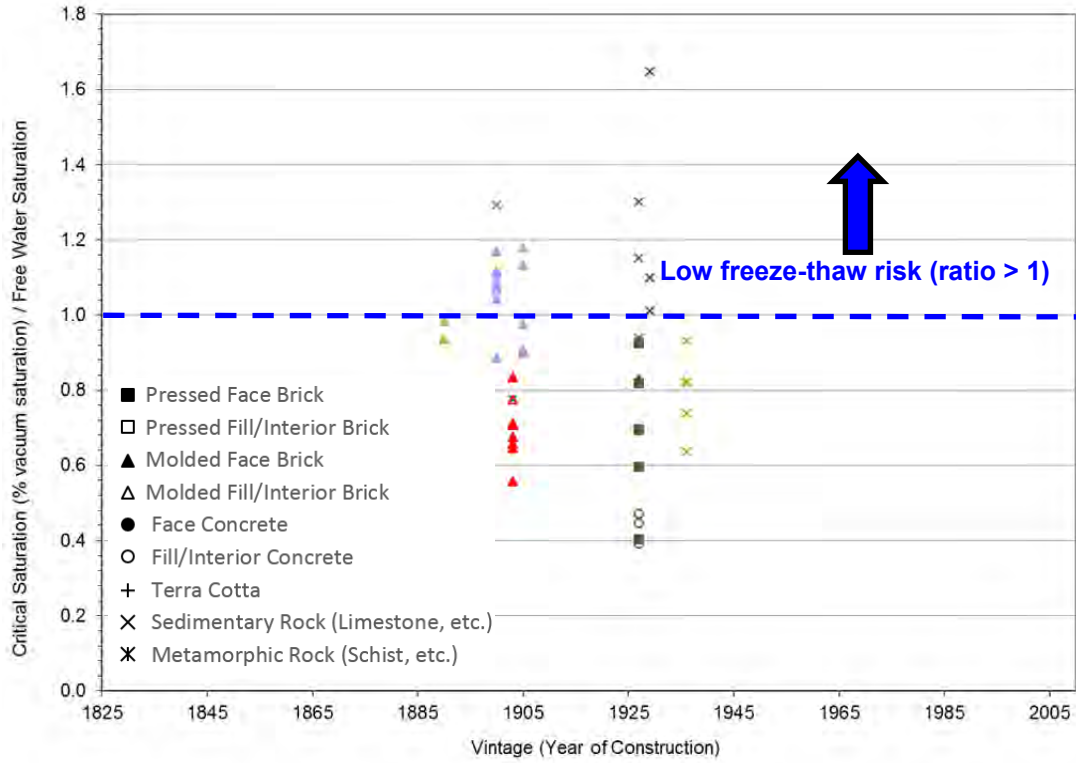


Figure 54: Critical degree of saturation as a fraction of Free Water Saturation vs. Vintage

## **Conclusions and Further Work**

Specific answers to the research questions from the test plan can be found in the final section of the report, “6. Research Question Answers and Further Work”

All measurements showed significant variation for some bricks from the same building, which are presumably of the same vintage, manufacturer, etc. Considering the variation in manufacturing for older bricks, it seems unlikely that generalizations based on brick characteristics determined by visible inspection will be a reliable assessment tool for assessing the freeze thaw degradation risk to a specific wall under a specific loading. However, this does not preclude drawing such information from the existing degradation (or lack thereof) of masonry in service under specific loading conditions.

There do not appear to be any obvious correlations between brick properties and vintage: in other words, knowledge of the vintage does not provide sufficient insight to eliminate the need for material property tests. Further development of test methods and masonry material properties databases is recommended in the hope that future review of larger data sets may identify other opportunities for generalization.

Comparisons between different projects and the same brick manufacturer were not shown due to a lack of clear evidence that any two projects used the same manufacturer’s bricks. Hence, the application of test results of an identified brick source from a previous project will not begin occurring until a substantial database of testing results has been populated.

Quantification of correlations has not been attempted for the dataset presented in this section. Generally, the sample sizes are too small to apply such methods to subsets of this dataset and hence, very poor correlation coefficients are anticipated. Further development and population of a masonry materials properties database may present such opportunities in the future.

## 4 Effect of Salts on the Durability of Masonry Materials

This section addresses the question of how salts affect the durability of masonry materials, and more specifically, how they affect assessments of freeze thaw degradation risk when adding interior thermal insulation to masonry buildings. Many masonry degradation phenomena are linked to salt content and/or movement, such as blistering, crumbling, efflorescence and subfluorescence, salt fretting/erosion, spalling, sugaring, and honeycomb weathering (NPS 1984).

### Background

Salts in masonry come from several sources including:

- a. De-icers and fertilizers directly deposited, deposited through melting snow and ice, or splashed de-icer-laden water from roads, pathways, stairs, etc. (see Figure 55 left). The resulting damage is known as salt fretting or salt erosion (NPS 1984);
- b. Salt-laden ground water wicking up through the wall (see Figure 55 right, Figure 56, and Figure 57);
- c. Salt and pollutant-laden air and mist; and
- d. Salt content within the construction materials (brick, mortar, mortar water).



**Figure 55: Suspected de-icer salt damage (left) and basement capillary rise damage (right)**

The presence of excessive salts from de-icer applications can be diagnosed during field visits by salt staining and/or damage adjacent to areas of application. These problems are best solved by limiting exposure to the de-icer compounds.



**Figure 56: Brick spalling and paint blow-off basement party wall due to capillary rise**

Ground water rising up through masonry walls and evaporating can deposit salts with damaging consequences (as described by Lstiburek 2007b; Figure 57).

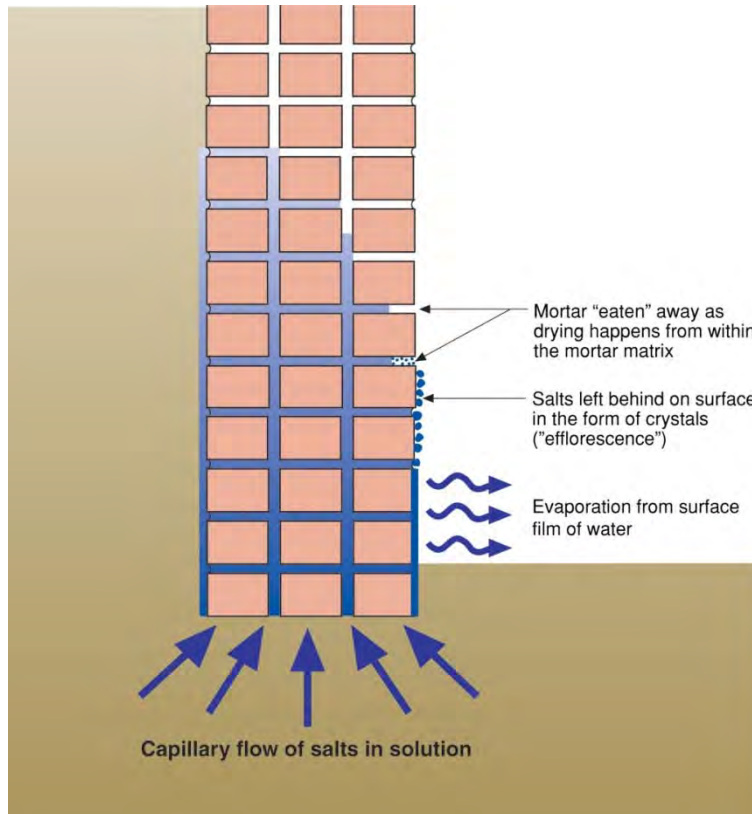


**Figure 57: Capillarity (“rising damp”) transport of salts, causing efflorescence (Lstiburek 2007b)**

The nature and severity of these deposits can change significantly with an interior thermal insulation retrofit. Similar to issues with de-icing salts, existing issues are diagnosed onsite by correlation with damp soil proximity; the solution is to limit exposure. A number of approaches to limiting exposure are available (Lstiburek 2007b) and should be considered when executing an interior thermal insulation retrofit.

Once de-icer exposure and/or ground water (“rising damp”) issues have been resolved, a residual amount of salts will be present in the masonry. Salts can also be present in significant quantities in old bricks, mortar, and from water used in the mortar mix. Air and mist can also carry salts and deposit significant quantities over time. The quantity of various salts in masonry is not readily discerned visually.

There is little published data on expected or measured salt concentrations of existing masonry assemblies. The most common salts in masonry are sulfates, chlorides, and nitrates (Perry and Duffy 1997). Ottosen et al. (2007) utilized an Austrian standard as “the only available source of threshold values at present” of the following percentages of Cl<sup>-</sup> (chloride ion).

- <0.03% (“no risk”)
- 0.03-0.1% (“individual evaluation necessary”)
- >0.1% (“active salt removal advised”)

This research team’s current protocols currently do not measure salt content as part of frost dilatometry measurement. However, this measurement is being added to the test protocol in future work; initial testing will include overall salinity measurements of ground masonry samples dissolved in water. Further lab testing would be required to determine specific salt chemistry, if this is considered useful information.



**Figure 58: Preliminary masonry sample salinity testing, with deionized water control samples**

This section includes a literature review exploring the potential impact of salts on our assessments.

### **Salt and Freeze Thaw Damage**

Considerable research on freeze thaw mechanisms and the impacts of salts on concrete were found in the literature focused on concrete. These sources all agree that de-icing salts exacerbate freeze-thaw damage. We assume these findings are generally applicable to other types of porous masonry.

The first measurements of the impact of de-icers (including salts) on concrete freeze thaw were by Verbeck and Klieger (1957). They subjected saturated concrete specimen with de-icer NaCl concentration of 0%, 2%, 4%, 8%, and 16% to repeated freeze thaw cycles. They found that

concentrations of salts up of 4 to 8% resulted in the highest severity of scaling of specimens. Later Fagerlund (1973) found peak damage at 3 to 5%. More recent testing by Lindmark (1996) places peak damage at 3%.

The role of these de-icers is thought to increase the effects of osmotic pressures (Fagerlund 1973). Osmotic pressure constitutes one of the theories of freeze thaw degradation. The osmotic freeze-thaw damage mechanism can be summarized by the following steps:

- Water within the porous material is recognized as having dissolved chemicals including salts, and these impurities reduce the freezing temperature of water.
- The freezing temperature is further reduced in smaller pores as a result of surface tension (independent of salt concentration); this phenomenon is characterized by the Kelvin equation (see Straube and Burnett 2005). Therefore ice forms first inside large pores.
- The formation of ice removes water molecules from the salt solution, so that the remaining solution (immediately next to the ice) has a higher salt concentration; osmotic pressures seek to equalize the salt concentration in all of the pores.
- Water is drawn from the small pores (where no water has frozen) to these large pores.
- The pressure in the large pores increases as a result of the addition of more water molecules.
- As more water molecules freeze, the mass of ice grows, the salt solution becomes more concentrated and more water molecules are brought to the freezing front by osmotic pressures
- The process accelerates, and the resulting internal stresses contribute to freeze thaw damage.

If the material is subjected to colder temperatures, more of the pores (i.e. a wider range of pore sizes) will freeze; however, there will always be some small pores that do not freeze so the damage mechanism can act over a wide range of freezing temperatures.

Another explanation was offered by Litvan (1975b), who concluded that the detrimental effects of de-icers can be attributed mainly to the higher degree of saturation. A higher degree of saturation occurs because the salt concentrations lower the saturation vapor pressure of the solution. This effect is balanced with a lowering of the freezing temperature. The result is that at very high salt concentration the lower freezing temperature dominates the process and detrimental effects decline.

The previous studies all measured freeze-thaw damage, as opposed to direct measurement of the critical degree of saturation ( $S_{crit}$ ). Hence, the direct effect of salt concentration on frost dilatometry testing is not covered in the literature.

Within our frost dilatometry approach, it is assumed that the samples are taken from the building with the current residual salt contents. Hence, if these salt contents were maintained, one could

suggest that the frost dilatometry testing captures their effects. However, this laboratory uses distilled water for water uptake testing and vacuum saturation prior to critical saturation testing. Such pre-tests could dilute the salt concentration within the samples, resulting in an inaccuracy. However, it is unknown if the salt content within masonry significantly affects critical saturation, or if the sample preparation process significantly affects this salt content.

Looking to the future development of such assessment, if our assessment were extended to predicting the extent of damage due to expected freeze thaw cycling above critical saturation levels, the whole process will need to be reviewed to ensure the severity of damage due to salts is captured. This is critical since it is clear that salt content affect severity of damage. However, it may also prove that salt contents are generally low enough not to have a significant impact.

### **Salt Damage**

Soluble salts are an agent of masonry decay apart from their effects on freeze thaw degradation. For instance, Garavaglia et al (2002) note: “Where freezing and thawing action is not present or not severe, the most important cause of damage is salt crystallization.” A summary of these effects is given by Woolfit (2000):

*The damaging effects of soluble salts are intimately linked with wetting and drying cycles at the masonry face. Almost all historic building materials are porous to some degree. The network of pores in stone and brick contain water in which varying quantities and types of salts may be dissolved. As drying/evaporation occurs at the masonry face, salts crystallize out of solution producing the white crystals known as efflorescence. While these fluffy white crystals can appear dramatic when projecting 10-20 mm from surfaces, they may be relatively harmless compared to hidden salt crystallization (cryptoflorescence) occurring within the pores below the masonry surface. Fine pores cannot accommodate the increasing accumulation of salts and are eventually broken apart by the expansive forces of crystal growth, causing the surface to decay.*

Crystallization pressures of salts in stone and concrete have been predicted to be as high as 67 MPa/9500 psi (Winkley and Singer 1972) lending support to this theory of salt induced decay; tensile strengths of brick are roughly an order of magnitude lower. However, the summary is an oversimplification: it has been found that “although salt damage has been intensively investigated for several decades, the mechanisms and factors that control the formation of salt crystals in porous building materials and the development of damage by crystal growth are poorly understood” (Pel et al. 2004). These developments will not be explored in this literature review; instead we are interested in the potential overlap of salt induced damage and our freeze thaw risk assessments.

As indicated, surface efflorescence is easy to diagnose, and can typically be safely cleaned without compromising the wall system. Sub-efflorescence (or subfluorescence), on the other, could be misdiagnosed as freeze thaw spalling based on visual inspection. The *International Centre for the Study of the Preservation and Restoration of Cultural Property Laboratory Handbook* (Borrelli 1999) stresses the importance of determining salt content of deteriorated surface to understand the causes of damage, and determine appropriate treatment.

Based on these insights, it has been concluded that an assessment of salt content should be considered for a scenario where the decay mechanism is unclear.

### **Moisture Transport and Storage**

In our analysis of the effect of retrofit interior insulation, we perform hygrothermal simulations to predict temperature and moisture conditions through proposed wall assemblies. These conditions are then post-processed to determine if moisture levels within the masonry will exceed the critical degree of saturation ( $S_{crit}$ ) at freezing periods. This simulation process is described in BSC (2012), in Chapter 8, “8 Assessment, Analysis, and Risk Management.” The most common software used in the industry for such analysis is WUFI. The program utilizes relative humidity as the driving force for moisture flows.

Koniorczyk and Gawin (2008) argue that such analysis is not well suited to assemblies with significant content of salts. This is because dissolved salt can strongly affect hygroscopic sorption and water retention characteristics, leading to more water retention. The authors do not provide salt contents at which these effects significantly affect hygrothermal behavior.

However, the WUFI model has been successfully validated with masonry assemblies monitored under real field exposure (Künzel and Holm 2009, Straube and Schumacher 2003). If salt effects and presence were significant, one would expect commensurate error. Alternately, the monitored wall assemblies might not have had sufficient salt content to significantly affect their performance.

It is uncertain where and when salt effects on moisture transport and storage will affect hygrothermal simulation.

### **Conclusions**

Specific answers to the research questions from the test plan can be found in the final section of the report, “6. Research Question Answers and Further Work”

Assessment and mitigation strategies for de-icer, fertilizer, and rising damp-related salt sources are well documented in the literature, and are already a standard part of field assessment. However, significant residual salts could (a) remain after such issues are addressed, (b) be present at time of construction or (c) be added via exposure air or mist-borne salts. The quantities of various salts in masonry are not readily discernible from visual field inspection.

Currently we do not measure salt contents in masonry samples tested in our laboratory, and cannot find data on similar masonry in the literature. Such testing should be considered and/or further investigation should be performed for sourcing such data.

The correlation between critical saturation levels and salt content are unknown. Unless it can be shown that salts contents have no effect, our testing procedure should be reviewed to ensure that salt contents are maintained for critical saturation testing.

It is known that salt content affects severity of damage. If our assessment were extended to predicting the extent of damage due to expected freeze thaw cycling above critical saturation levels, the whole process will need to be reviewed to ensure the severity of damage due to salts is captured.

Considering that salt decay is also a significant contributing mechanism for masonry decay, a methodology should be developed to ensure sub-surface efflorescence (subfluorescence) damage is not confused with freeze thaw damage during our field assessments. Some cases can clearly be differentiated visually, but other cases may be less clear. This could tie in with salt content testing as part of our laboratory or field testing. The field assessments might provide insight as to whether subfluorescence is a significant problem in the existing and/or retrofitted building stock.

Furthermore, it is unclear if interior insulation retrofits can cause or exacerbate significant salt decay for walls, due to changes in temperature regime and/or drying magnitude or direction. Additional exploration may be warranted.

## 5 Optimization of Freeze Thaw Dilatometry Testing

The frost dilatometry (freeze-thaw test) process often has to be repeated, and has significant time and cost requirements. This section examined optimizations to testing methods, determining whether they had any detrimental effects on measurements.

### Introduction

The basic methodology for using frost dilatometry to determine the critical degree of saturation ( $S_{crit}$ ) and freeze-thaw resistance of masonry materials has been described in previous work (Mensinga et al. 2010; Schumacher 2011). Although these methods are currently used in practice, minimizing the time and cost requirements for such testing would allow more thermal insulation retrofit projects to benefit from frost dilatometry.

The current approach to frost dilatometry testing involves the following major steps:

1. Cut “slices” from sample bricks for testing,
2. Saturate sample slices to a desired overall moisture content,
3. Wrap slices in plastic to minimize drying and maintain moisture content,
4. Allow the moisture content to equalize throughout the sample,
5. Measure the pre-test length of sample slices cut from units (and re-wrap),
6. Subject the sample to several freeze thaw cycles, and
7. Re-measure the sample length to determine dilation (growth).

This method is recommended because some materials undergo sufficient moisture expansion to increase uncertainty in measurements, when the pre-test length is measured dry (as covered later in this section).

Optimizations covered in this research includes reduction of the sample sizes (“slices”), improving the process of sample length measurement, and reducing freeze-thaw cycle time.

### Reduced Sample Sizes

The sample slices used in our critical saturation testing have typically been 2” x 3 ½” x 3/8” (50 x 89 x 10 mm). The 3/8” (10 mm) thickness was as thin as we were comfortable cutting. The 3-½” (89 mm) length fits the commonly available 3-4” (76-102 mm) micrometer, and is long enough that significant damage causes measurable strain. The width was based on typical brick sizes where the top and bottom were cut to square.

As part of this exercise, the width was identified as a non-critical dimension. An opportunity was identified to reduce this dimension to 1” (25 mm) without negatively affecting the testing. A photo of the old and new samples is provided in Figure 59. This allowed twice as many slices to fit into the controlled temperature bath for freeze thaw cycling, thus doubling the throughput.

It also allows twice as many samples to be taken from sample bricks, which is useful in some cases due to sample availability.



**Figure 59: New (top) and old (bottom) brick slice samples**

### **Sample Length Measurement**

Critical degree of saturation (or  $S_{crit}$ ) is determined by subjecting samples to freeze-thaw cycling at various moisture contents (% vacuum saturation). At or above the  $S_{crit}$  value, the sample grows or dilates after cycling. However, the dilation is very small, often on the order of 200 to 3000 microstrain. One microstrain is one part per million ( $10^{-6}$ ), so 1000 microstrain would be a dilation of 0.1%. The accuracy of sample length measurements before and after the freeze thaw cycling determines the uncertainty of strain and hence, critical saturation measurements.

Furthermore, it sets a lower limit of resolving sample dilation, as shown by the scatter in Figure 60. When such low microstrains are found after freeze thaw cycling, the samples must be exposed to further freeze thaw cycling, in order to “draw” out greater strains (allowing better estimation of critical saturation).

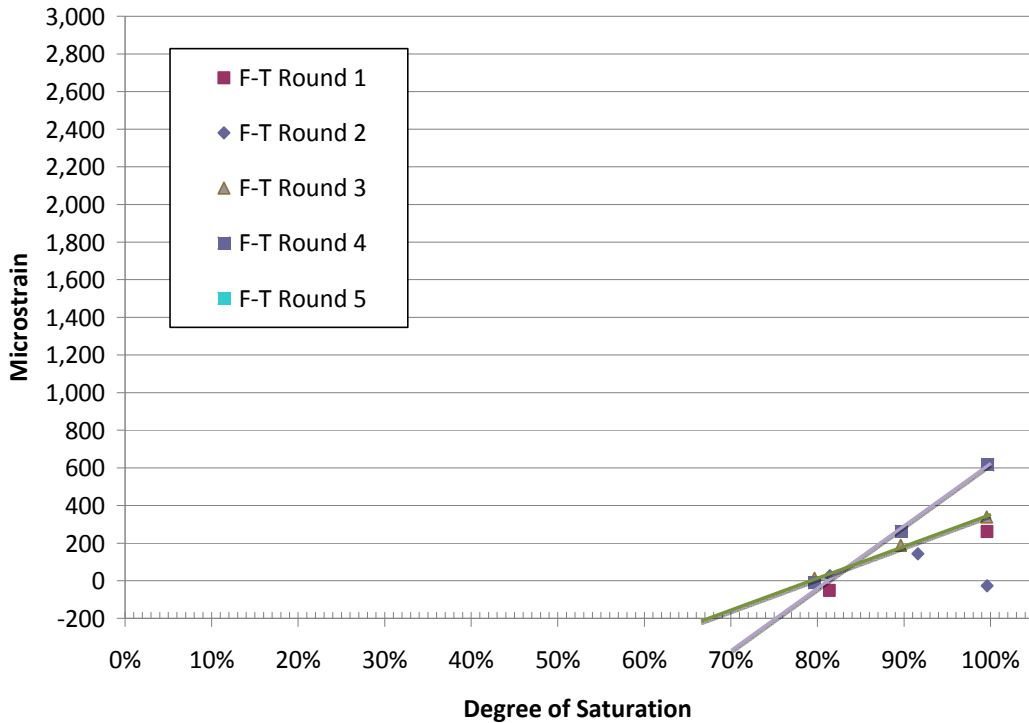


**Figure 60: Freeze thaw testing results for New England circa 1900 brick samples**

Metal targets were used by Mensinga et al. (2010), as illustrated in Figure 61, in order to improve length measurement accuracy. Photos of such a sample are also included in Figure 61. These targets are added to ensure that the length of the slice is taken at the same place repeatedly.

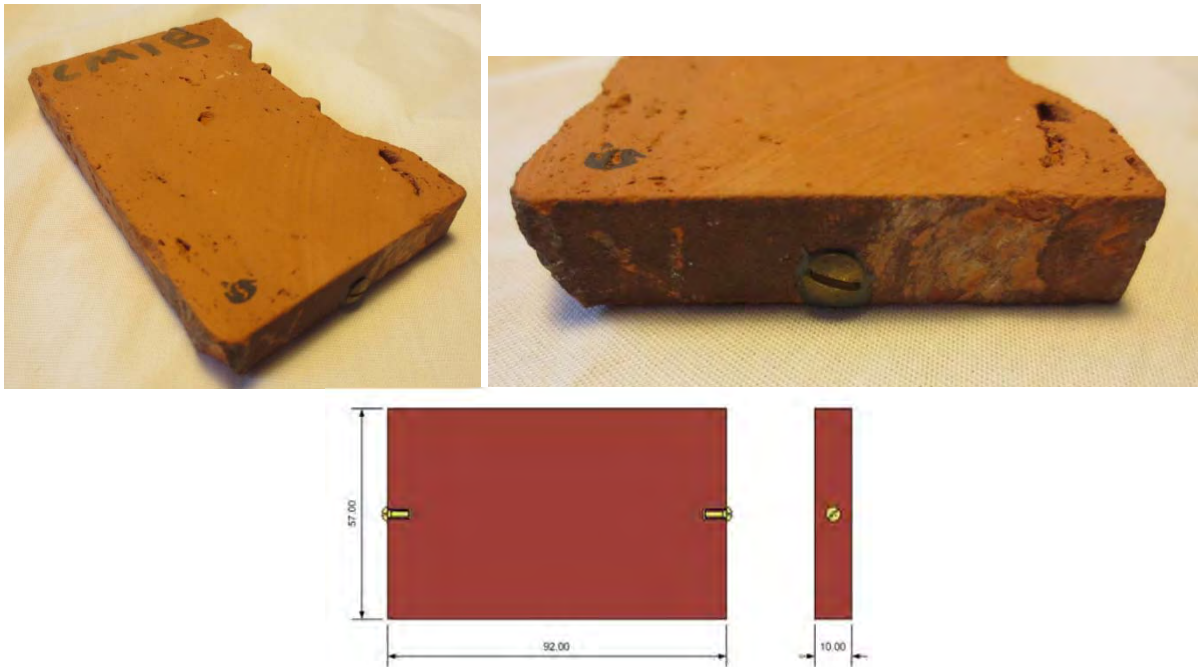


**Figure 61: Photo and illustration of sample brick slice with metal screw targets**

The installation of targets and waiting for their epoxy to set is a time consuming process. A test was done where length measurements were repeated for samples with and without the metal targets. The results, given in Table 1, suggest that the use of set screws provide a fairly consistent standard deviation. The measurements for the samples with the metal targets show standard deviations of 63 to 81 equivalent microstrain. Without the metal target measurements, this standard deviation range increases to 54 to 165 equivalent microstrain.

**Table 1: Repeated length measurements (inches) of brick slices without jig**

Measurement #	No jig with metal targets			No jig without metal targets		
	Sample 1	Sample 2	Sample 3	Sample 4	Sample 5	Sample 6
1	3.4955	3.6113	3.6201	3.5430	3.3699	3.3793
2	3.4949	3.6115	3.6202	3.5434	3.3701	3.3795
3	3.4950	3.6117	3.6200	3.5425	3.3702	3.3789
4	3.4954	3.6111	3.6205	3.5428	3.3698	3.3790
5		3.6116	3.6205	3.5419	3.3698	3.3782
Mean	3.4952	3.6114	3.6202	3.5427	3.3699	3.3790
Standard deviation	0.000284	0.000228	0.000231	0.000586	0.000182	0.000497
St Dev/Mean * 10 <sup>6</sup>	81	63	64	165	54	147

In order to achieve greater repeatability of length measurements without the use of the metal target screws, a jig was constructed to ensure that the samples would be measured repeatedly in the same location. The intent was also to limit the variability in measurement repeatability due to the operator. Sample measurement with and without the jig is shown in Figure 62. The results of a small set of repeated tests are given in Table 2, which can be compared with the results from Table 1. The repeatability of the measurements is significantly better than the earlier measurements with the metal targets. The measurement variability is also approaching the intrinsic precision of the micrometer ( $\pm 0.00005''$ ). Hence, the use of jig without the set screw was adopted to minimize costs (associated with sample preparation time) while maintaining or improving repeatability.

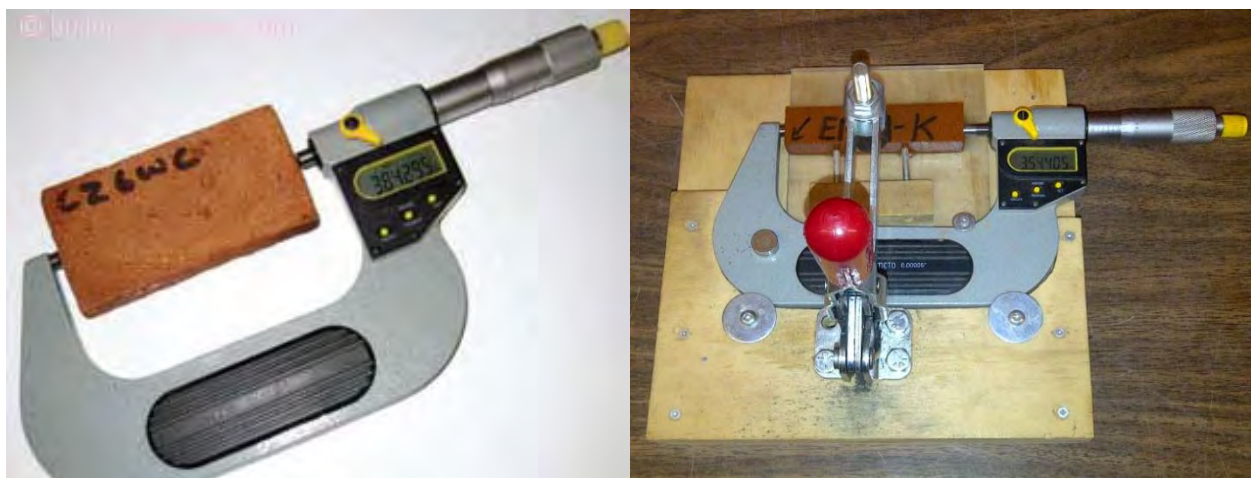


**Figure 62: Strain measurements with (right) and without jig (left)**

**Table 2: Repeated length measurements (inches) of brick slices with jig**

Measurement #	Jig without metal targets		
	Sample 7	Sample 7	Sample 9
1	3.5891	3.5868	3.5402
2	3.5891	3.5867	3.5401
3	3.5891	3.5868	3.5401
4	3.5891	3.5868	3.5401
5	3.5891	3.5867	3.5402
Mean	3.5891	3.5867	3.5401
Standard deviation	0.000022	0.000055	0.000067
St Dev/Mean * 10 <sup>6</sup>	6	15	19

Repeatability issues were suspected in projects prior to the development of the measurement jig described above. A further study was conducted to quantify the repeatability of our measurements. The repeatability of the brick slice length measurements sets the minimum amount of strain needed for determining that strain has actually occurred (as opposed to measurement/repeatability error), and therefore the precision of our critical saturation measurements.

It was observed in the study that some brick samples can be measured many times with repeatability, while other samples will measure smaller each time they are measured, up until a certain number of measurements, when this effect stops. This effect seemed to be related to the “softness” of the bricks, although we did not measure sample hardness. As seen in Figure 63, a typical 'soft' brick showed a measurement decay of approximately 30 microstrain per measurement for the first 4 measurements, with decay slowing after the fourth. Anecdotal evidence shows that this pattern is typical, with the decay occurring over the first 3 to 10 measurements.

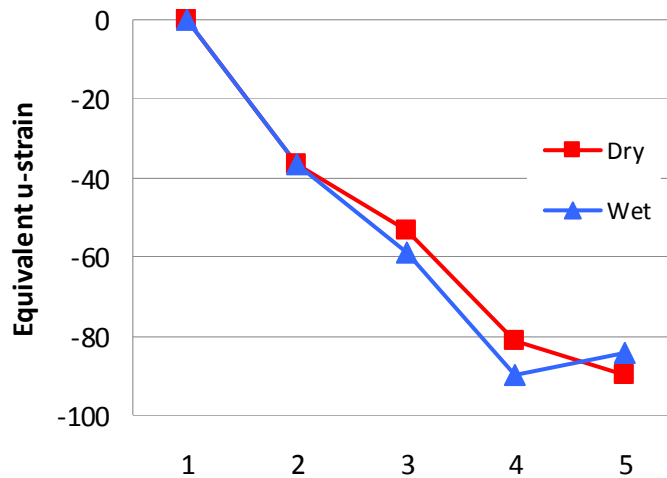


**Figure 63: Average measurement decay over 5 consecutive measurements for 5 slices on one 'soft' brick sample**

If an average of the first 5 measurements is used as the initial length, this would result in an artificially inflated initial measurement, making future dilation (growth) hard to determine. Similarly, if an average of the first 5 measurements is used as the post-freeze-thaw measurement,

an artificially small measurement would result, which could hide actual freeze-thaw growth (frost dilation)

To minimize these effects, some additional measurement protocols were developed. For initial measurements, the first five consecutive measurements with a total change of less than 0.00020 inches were to be used. For post freeze-thaw measurements, only the first measurement should be used, provided that a second measurement is no more than 0.00050 inches different than the first.

Specifically for the 'soft' bricks mentioned above, it has been observed that slice length measurements decrease significantly after the slices have been soaked in water. As seen in Figure 64, for the 5 samples tested, the average measurement was reduced by 500 to 2000 microstrain after being soaked in water. The variation resulting from this effect is dramatically greater than the previously mentioned effects, and can be a major source of error.

To minimize the variability resulting from this effect, all initial measurements now are taken after being brought to test water saturation level and left to settle for at least 1 hour.

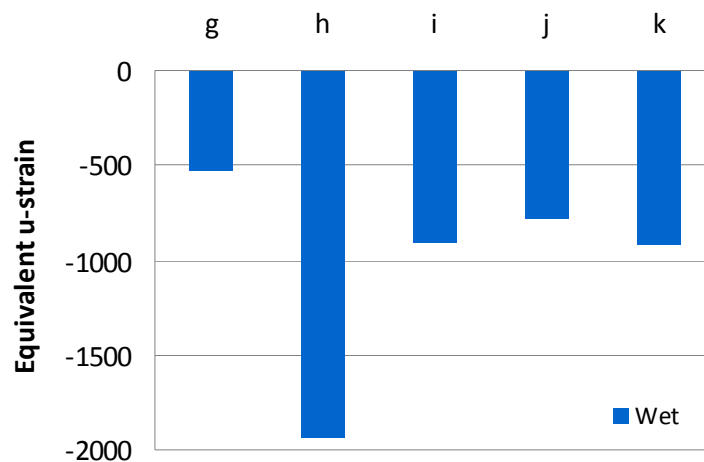


**Figure 64: Difference in average microstrain measurements of 5 'soft' brick slices after soaking in water for 1 hour relative to dry length (no freeze thaw cycles)**

With the soft brick issues previously discussed addressed, operators showed a variability in measurement of 7 to 43 micro strain. When the same 6 brick slice samples were measured by two different operators (labeled “Measurer X” and “Measurer Y” in Table 3), variability of 0 to 59 microstrain was found for 4 of the samples, and 204 for one outlier. Upon investigation, it was discovered that this sample was not cut square, and that the operator variance in loading the sample was likely the cause of the variance. We currently apply 200 microstrain as the measurement uncertainty (minimum level for indicating dilation) when assessing critical saturation.

**Table 3: Repeatability measurement (inches) after addressing ‘soft’ brick issue**

<b>Measurer X</b>					
Measurement #	Sample 1	Sample 2	Sample 3	Sample 4	Sample 5
1	3.0618	3.0591	3.0621	3.0435	3.0417
2	3.0617	3.0591	3.0619	3.0436	3.0417
3	3.0616	3.0590	3.0618	3.0438	3.0417
4	3.0620	3.0590	3.0619	3.0437	3.0417
5	3.0617	3.0589	3.0620	3.0437	3.0417
Mean ( $\bar{X}$ )	3.0618	3.0590	3.0619	3.0436	3.0417
Standard deviation	0.00013	0.00010	0.00011	0.00010	0.00002
St Dev/Mean * 10 <sup>6</sup>	43	32	37	34	7

<b>Measurer Y</b>					
Measurement #	Sample 1	Sample 2	Sample 3	Sample 4	Sample 5
1	3.0617	3.0590	3.0618	3.0442	3.0417
2	3.0617	3.0590	3.0619	3.0444	3.0417
3	3.0617	3.0590	3.0617	3.0443	3.0416
4	3.0615	3.0590	3.0617	3.0442	3.0416
5	3.0617	3.0590	3.0618	3.0443	3.0416
Mean ( $\bar{Y}$ )	3.0616	3.0590	3.0618	3.0443	3.0416
Standard deviation	0.00008	0.00003	0.00007	0.00008	0.00004
St Dev/Mean * 10 <sup>6</sup>	27	9	21	26	14

<b>Comparison</b>					
$(\bar{X} - \bar{Y}) / \bar{X} * 10^6$	36	0	59	-204	16

Several opportunities were identified and implemented to reduce the uncertainty of dilation measurements and to reduce testing costs and time requirements. These included:

- Replacing the use of metal targets with the use of a positioning jig, resulting in a net increase in accuracy
- Adopting an initial measurement routine of repeated measurements until a consistent length measurement is found (due to “soft brick” erosion issues); and
- Measuring samples at test (“wet”) moisture contents

### Freeze-Thaw Cycle Time Improvement

Freeze thaw cycle time is the major critical path time constraint in laboratory testing for frost dilatometry. For small laboratories it also is a resource constraint, as they will likely only have one chilled bath (see Figure 65). Both considerations add cost to this testing, which constrains adoption of the methodology on a wider scale. An opportunity was identified to compress cycle schedules.



**Figure 65: Chilled bath (Schumacher 2011)**

It is generally accepted that increasing cooling rate increases freeze thaw damage (Lindmark 1996). However, it has been shown that cooling rates do not significantly affect critical saturation measurements (Fagerlund 1992). We confirmed this for one set of brick samples by laboratory testing. Three bricks samples were cut into slices. These slices were vacuum saturated and then dried to different saturation levels. For round #1, the samples were cooled from 10°C/50°F to -15°C/5°F over a 1 hour period. For round #2, the cooling rate was over a slower 3 hour period (using different slices from the same bricks). The results plotted in Figure 66 through Figure 68 confirm that the cooling rate did not significant affect the critical saturation measurements for the tested bricks. Hence, modification of cooling rate within these bounds was considered acceptable.

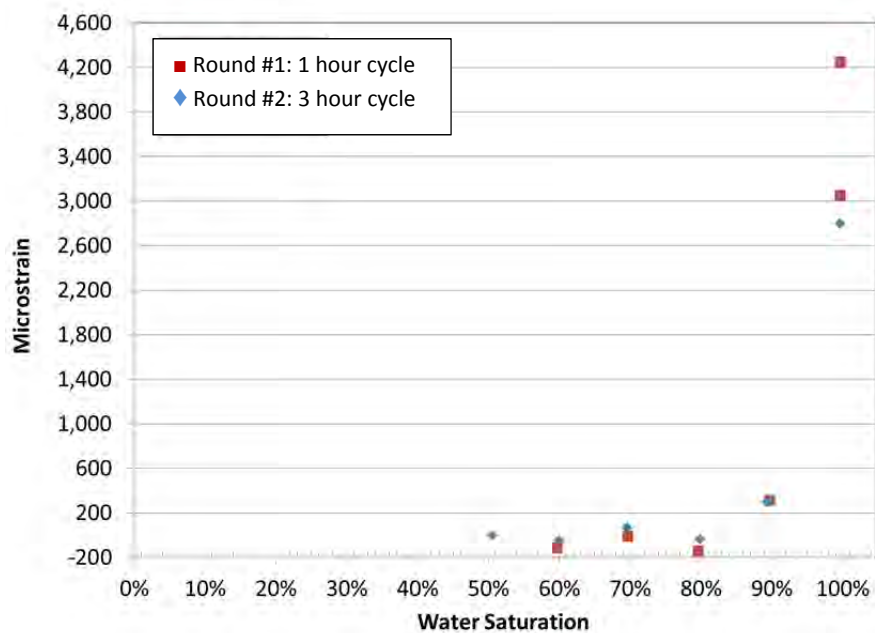


**Figure 66: Sample 1 - Permanent microstrain measured after 15 freeze thaw cycles**

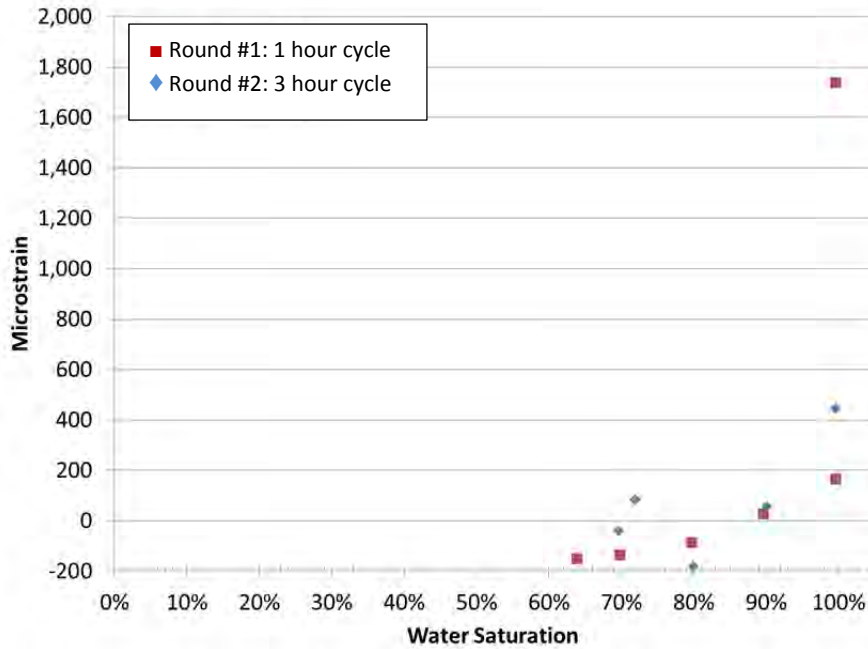


**Figure 67: Sample 2 - Permanent microstrain measured after 15 freeze thaw cycles**

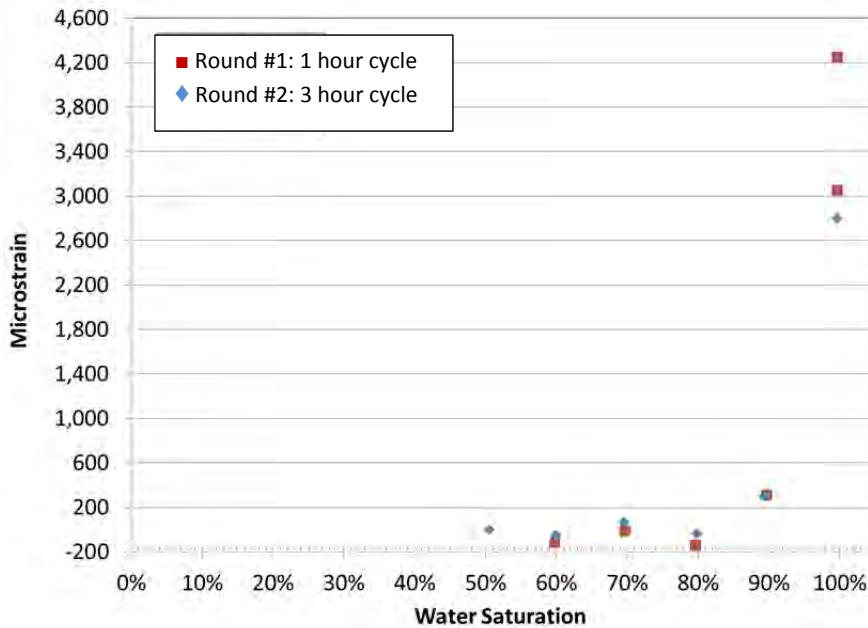


**Figure 68: Sample 3 - Permanent microstrain measured after 15 freeze thaw cycles**

It is also generally accepted that a lower temperature also increases freeze thaw damage (Lindmark 1996). In the current protocol, the samples are cooled to  $-15^{\circ}\text{C}/5^{\circ}\text{F}$  because a) it is a lower temperature than occurs in the field for typical New England projects, and b) it is similar to the temperature which must be achieved at the center of specimens in the ASTM C 666 (ASTM 2008) test. Modification of minimum freezing temperature was maintained for the cycle time compression.

The original freeze-thaw cycle schedule is shown in Figure 69. Samples are cooled from 20°C/68°F to -15°C/5°F over a 2 hour period, held for 1 hour, thawed over a two hour period to 20°C/68°F, and held for 1 hour before being repeated. It was identified that the thaw temperature did not need to be 20°C/68°F. We also knew that the cooling rate could be increased from literature and previous testing. The resulting increase in damage from an accelerated cooling rate is advantageous for our methodology, because greater dilation results in more accurate critical saturation measurements.

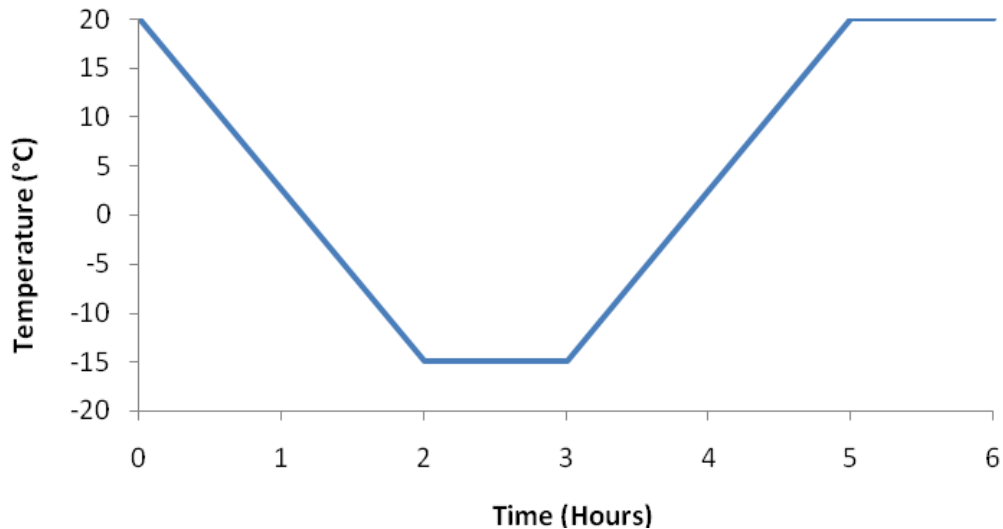


**Figure 69: Freeze thaw testing typical cycling time**

The 1 hour hold times were originally set to ensure that the sample was completely thawed or frozen to -15°C/5°F. In order to ensure that the target temperatures was reached at the brick samples core, a thermistor was installed within the core of a sample slice (Figure 70).



**Figure 70: Thermistor installed within brick slice**

In order to measure the temperature accurately at the core of the slice, a hole was drilled in the end of the slice reaching the center. The hole was drilled along the longest axis to minimize

thermal conductivity effects of the thermistor wire and cable. We then measured core temperature during freeze-thaw cycling of a sample within the middle of a full load of samples in the chilled bath.

Plots of slice core temperatures are given in Figure 71 for the initial original schedule and the modified schedule. The core temperature of the sample slice closely follows the bath temperature.

A slight jog in the temperature occurs when the temperature crosses 0°C/32°F. This is due to the latent heat capacity of the water within the sample. This jog is not evident in the modified cycling routine; this is likely due to secondary factors, such as (a) dryer samples, with lower moisture contents, (b) fewer slices in the chilled bath, which increases the bath’s effective cooling power, and (c) a change in chilled bath coolant chemistry.

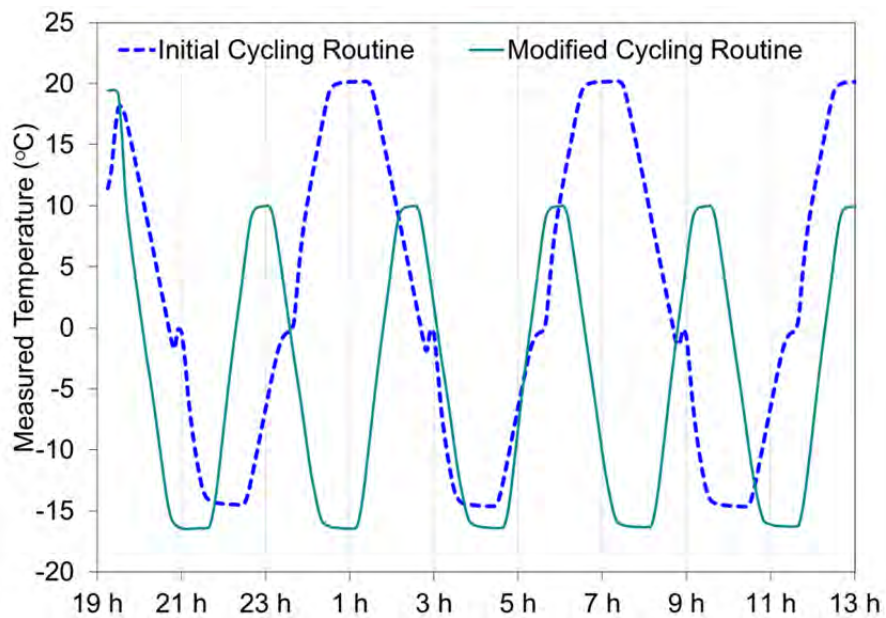


**Figure 71: Measured slice core temperature with initial and modified cycling routine**

The measurements demonstrate that by increasing the cooling rate, decreasing the target thaw (upper) temperature, and decreasing the hold time from an hour to 30 minutes, the cycling time can be reduced by almost half, without any loss in accuracy.

## 6 Research Question Answers and Further Work

The answers to the research questions are divided by section, followed by opportunities for further work in this field. The research questions are stated in italics. The full set of conclusions for each research topic can be found in the corresponding section of this report.

### Field Monitoring of Embedded Wood Members in Insulated Masonry Walls

The associated research questions were as follows:

- *What are the temperature conditions at the joist pockets or beam pockets with and without retrofitted interior insulation?*

The difference between insulated and uninsulated conditions will be determined once the three compared insulation strategies (insulated with fiberglass, insulated with XPS and air sealed, uninsulated) are run with heated interior wintertime conditions.

- *What are the measured seasonal moisture contents of embedded beams in insulated and uninsulated cases, and can these be mapped to durability risks?*

Patterns of seasonal moisture contents will be determined once additional data are collected, past this initial 3-month winter window (under mostly unheated interior conditions).

- *Does orientation have a specific effect of temperature and moisture conditions? This will include both the effects of solar gain and wind-driven rain.*

Orientation appears to have a very strong effect on joist end moisture content, especially when the interior is unheated. Sides with strong solar heating, such as the south side, have low (10-15%) moisture contents, while sides with minimal solar gain (north, and shaded east) have much higher moisture contents (25-30%+). Driving rain exposure may also play a role, although localized rain concentrations (e.g., gutter runoff) could easily overwhelm differences in driving rain deposition.

- *Does distance from grade (“rising damp” via capillary activity) have a specific effect on temperature and moisture conditions?*

Insufficient data exist so far to determine differences between the basement ceiling-level joists and the first floor ceiling-level joists. In addition, the difference in elevation cannot be disaggregated from the fact that the construction type is different between these two floors. The basement level wall is solid brick masonry, and the first floor level is hollow clay block backup wall.

- *Is there a significant difference in the performance of an insulated beam without an air seal around the beam pocket, compared to one that is rigorously air sealed?*

Based on the preliminary data, the effect of completing the air seal at the perimeter of the embedded joist only had a small effect. However, this is based on limited before/after air

seal data, with interior conditions only at 50-60° F and low humidity. This behavior would be vastly different under occupied (and especially humidified) interior conditions.

- *Are there measurable airflows occurring at joist pockets in wintertime or summertime conditions? Given the limits of hot wire anemometers, it is unlikely that it is within the measurement range, but will be checked for reference.*

Airflows were not measurable with available equipment.

- *How do the monitored data correspond to previous three-dimensional and one-dimensional simulations?*

Correlations between monitored data and simulations will be determined once additional data (e.g., a full year of conditioned operation with insulated and air sealed joists) have been collected.

### **Use of General Masonry Characteristics and Basic Materials Testing**

The associated research questions were as follows:

- *Based on analysis of the existing database of masonry material property testing results, can freeze-thaw resistance generalizations be made based on easily discernible properties, such as vintage, geographic location, brick type (pressed vs. extruded), porosity, etc.?*

The database of 24 previous projects was analyzed to determine whether generalizations could be made based on easily observable characteristics. Various material properties, including dry density, porosity, water uptake, free water saturation, and critical degree of saturation ( $S_{crit}$ ) were plotted against other variables, including vintage. Little correlation could be determined from these plots, including factors such as brick manufacturing type and geographic location.

In addition, all measurements showed significant variation for some bricks from the same building, which are presumably of the same vintage, manufacturer, etc. Considering the variation in manufacturing for older bricks, it seems unlikely that generalizations based on brick characteristics determined by visible inspection will be a reliable assessment tool for assessing the freeze thaw degradation risk to a specific wall under a specific loading.

### **Effect of Salts on the Durability of Masonry Materials**

The associated research questions were as follows:

- *What is the theoretical impact of salts in masonry materials?*

Based on the literature on concrete masonry freeze-thaw damage and salts, de-icing salts exacerbate freeze-thaw damage. This impact has a maximum at concentration ranging from 3 to 8% (NaCl solution strength by weight). It is assumed that similar effects would take place in masonry as researched in concrete.

- *How might dissolved salts affect the mechanics of freeze-thaw?*

There are multiple theoretical explanations of the mechanics of the impact of salts on freeze-thaw. Most of them concur, however, that osmotic pressures (pressure drives due to different salt concentrations) affect the movement of water when ice is formed. These osmotic pressures can be sufficient to create internal stresses that exceed the tensile strength of masonry materials, causing damage (spalling or scaling).

- *What range of osmotic pressures might be expected? Could these pressures result in damage?*

Osmotic pressures have been reported in the 21 MPa/3000 psi range; this is an order of magnitude higher than typical tensile strengths of brick or other masonry materials.

- *What are the mechanics of subfluorescence?*

Liquid water moving by capillarity (“wicking”) through porous masonry materials can carry dissolved salts with them. When the salts reach the surface and the water evaporates, the salt will recrystallize, resulting in surface deposits (efflorescence). However, this phenomenon is principally cosmetic and not harmful. On the other hand, if the salt recrystallizes within the pores below the masonry surface, subfluorescence (or sub-efflorescence, or cryptofluorescence) will result. These two phenomena may be coincident (e.g., surface efflorescence suggests that subfluorescence may be occurring), but not necessarily linked. The expansive force of salt crystal growth can be significant (67 MPa/9500 psi range), and can overcome the tensile strength of masonry materials, thus causing spalling.

- *Do practitioners confuse freeze-thaw damage and salt damage in the field?*

Given the surface spalling or scaling that is common to both freeze-thaw and salt damage, it seems likely that they may be confused in the field. Preservation and restoration resources recommend determining salt contents of deteriorated surfaces to ascertain whether one or another phenomenon is the root cause.

### **Optimization of Freeze Thaw Dilatometry Testing**

The associated research questions were as follows:

- *Can targets (metal reference points attached to the sample, similar to those used in structural testing) be used to improve repeatability of dimension measurements?*

Metal reference points (screws epoxied into sample ends) were used in the original length measurement work; however, it was found that they added sample preparation time. A faster measurement method that improved repeatability was to use a clamping jig, which fix the sample and calipers in a consistent orientation.

- *Is there an alternative to measuring dimensions; for example, can freeze-thaw damage be identified via acoustic methods such as measurements of attenuation?*

Alternate measurement methods were not researched, given the improvement in throughput achieved with the existing frost dilatometry method.

- *Can the freeze-thaw cycle be modified in order to decrease test cycle time, and therefore increase throughput? AND*
- *Alternately, could the cycle time be compressed to allow more freeze-thaw cycles and a greater dilation to be achieved in a shorter time period?*

The cycle was decreased to almost half (doubling the throughput), without any loss in accuracy. This was achieved by increasing the cooling rate, decreasing the target thaw (upper) temperature, and decreasing the hold time from an hour to 30 minutes.

- *Are the temperatures & time steps currently used sufficient to bring the entire masonry specimen (including the core) to target temperatures*

Temperature measurements of the core of the sample demonstrated that the accelerated freeze-thaw cycle described above will achieve full temperature penetration into the core of the sample (by comparison with chilled bath temperature).

### **Further Work**

Further opportunities for research work (based on the research to date) are broken down by topic below.

#### ***Field Monitoring of Embedded Wood Members in Insulated Masonry Walls***

The intent is to continue data collection at this monitoring installation over time, to provide insight into the long-term durability of the interior insulation retrofit. For instance, it is expected that during warmer summertime weather, the moisture content in the joist end will fall. On the other hand, summertime often has high levels of precipitation; the response (if any) of the joist end moisture content to wind-driven rain events will be examined.

As noted above, the currently proposed renovation completion date is as late as December 2014, which leaves a substantial period before completed and occupied (i.e., heated) conditions occur. This suggests that relatively long-term monitoring may be needed to draw useful conclusions.

A key observation planned for the long-term monitoring is whether the seasonal moisture cycling results in a net increase in moisture levels over time, or “ratcheting.” This behavior would tend to indicate long-term durability risks, especially if moisture levels are rising to levels consistent with mold growth and rot for wood members.

If certain monitored locations are observed to have consistently high moisture levels, the building owners will be informed, and intrusive disassembly may be performed to determine the source of the moisture issues.

One suggested explanation for the higher moisture contents at the “lower” joist location is migration of salts from the masonry into the wood, which would increase apparent moisture

content due to electrical conductivity changes. If additional work can be budgeted, spatial differences salt content can be examined by analyzing drilled wood shavings.

### ***Use of General Masonry Characteristics and Basic Materials Testing***

The database of 24 previous projects was analyzed to determine whether generalizations could be made based on easily observable characteristics. However, relatively few useful patterns could be discerned from this database.

The addition of further test samples to the database may increase the knowledge base that can be used to make generalizations in the future. However, given the degree of variability in the measured results to date, it is unlikely that generalizations can be made based on brick manufacturing method, vintage, geographic location, or other characteristics.

### ***Effect of Salts on the Durability of Masonry Materials***

The current laboratory protocol does not include the measurement of salt contents in masonry samples, as received from the field. This testing is being incorporated into future measurements, and further investigation should be performed for sourcing additional data.

The correlation between critical degree of saturation ( $S_{crit}$ ) levels and salt content is unknown. Unless it can be shown that salts contents have no effect, the testing procedure should be reviewed to ensure that salt contents are maintained for critical saturation testing.

Considering that salt decay is also a significant contributing mechanism for masonry decay, a methodology should be developed to ensure sub-surface efflorescence (subfluorescence) damage is not confused with freeze thaw damage during field assessments. Some cases can clearly be differentiated visually, but other cases may be less clear.

Furthermore, it is unclear if interior insulation retrofits can cause or exacerbate significant salt decay for walls, due to changes in temperature regime and/or drying magnitude or direction. Additional exploration may be warranted.

### ***Optimization of Freeze Thaw Dilatometry Testing***

The work discussed here has resulted in improvements in throughput (reducing required laboratory time) and repeatability of frost dilatometry measurements. It is entirely possible that additional optimization may be possible; however, further modifications to the testing protocol are not evident at this time. Possible modifications may become evident during further laboratory testing.

Another potential research path is to explore whether acoustic methods (i.e., signal attenuation) are a viable alternative to length measurements used in frost dilatometry.

## References

[ASHRAE] American Society of Heating, Refrigerating and Air-Conditioning Engineers. (2009). *2009 ASHRAE Handbook—Fundamentals*. Atlanta, GA: American Society of Heating, Refrigerating and Air-Conditioning Engineers, Inc.

[ASTM] American Society for Testing and Materials. (2008), *ASTM Standard C 666, Standard Test Method for Resistance of Concrete to Rapid Freezing and Thawing*. ASTM International, West Conshohocken, PA.

[ASTM] American Society for Testing and Materials. (2009), *ASTM Standard C 67, Standard Test Method for Sampling and Testing Brick and Structural Clay Tile*. ASTM International, West Conshohocken, PA.

Borrelli, E., (1999). *International Centre for the Study of the Preservation and Restoration of Cultural Property Laboratory Handbook – Salts*. ICCROM/UNESCO/WHC, Rome.

[BSC] Building Science Corporation (2011). Building America TO2 Task 1.3: “Recommended Approaches to the Retrofit of Masonry Wall Assemblies: Final Expert Meeting Report.” ([http://www.buildingscienceconsulting.com/services/documents/file/BSC%20TO2%201\\_3%20Final%20Expert%20Meeting%20Report.pdf](http://www.buildingscienceconsulting.com/services/documents/file/BSC%20TO2%201_3%20Final%20Expert%20Meeting%20Report.pdf)) Somerville, MA: Building Science Corporation.

[BSC] Building Science Corporation (2012). Building America TO2 Task 7.3: “Internal Insulation of Masonry Walls: Final Measure Guideline.” (<http://www.buildingscience.com/documents/dcreports/dc-1105-internal-insulation-masonry-walls-final-measure-guideline/>) Somerville, MA: Building Science Corporation.

Charola, A. (2000) “Salts in the Deterioration of Porous Materials: An Overview.” *Journal of the American Institute for Conservation*, Vol. 30., No 2, Art 2.

Clemson University. (2013) “The Bishop Materials Laboratory.” [www.clemson.edu/mse/cd/brosnan.pdf](http://www.clemson.edu/mse/cd/brosnan.pdf)

Dumont, R., Snodgrass, L., et al., (2005) “Field Measurement of Wood Moisture Contents in Wood Joists Embedded in Masonry Exterior Walls.” *Proceedings of the 10th Annual Conference on Building Science and Technology*. Ottawa, ON.

Fagerlund, G., (1973) *Significance of critical degrees of saturation at freezing of porous and brittle materials* contribution to ACI-Symposium Durability of Concrete, Ottawa, ON.

Gonçalves, M.D. (2003). “Insulating Solid Masonry Walls.” *Ninth Conference on Building Science and Technology*, Ontario Building Envelope Council, Vancouver, BC, pp. 171-181.

Hudec, P., (1991). “Freezing or Osmosis as Deterioration Mechanism of Concrete and Aggregate?” *Low Temperature Effects on Concrete Second Canada/Japan Workshop*, Institute for Research in Construction, Ottawa, ON.

- Hughes, R., and B. Bargh, (1982). “The Weathering of Brick: Causes, Assessment and Measurement.” *A Report of the Joint Agreement between the U.S. Geological Survey and the Illinois State Geological Survey*.
- Hutcheon, N.B. (1964). NRC-IRC (Institute for Research in Construction) Canadian Building Digest CBD 50. "Principles Applied to an Insulated Masonry Wall." Ottawa, ON: National Research Council of Canada.
- Künzel, H. (1995). “Simultaneous Heat and Moisture Transport in Building Components: One- and two-dimensional calculation using simple parameters.” Ph.D. Thesis, Fraunhofer Institute for Building Physics. Holzkirchen, Germany.
- Künzel, H. (2002). WUFI® PC-Program for calculating the coupled heat and moisture transfer in buildings. Fraunhofer Institute for Building Physics. Holzkirchen, Germany.
- Künzel, H., A. Holm. (2009), Moisture Control and Problem Analysis of Heritage Constructions PATORREB 3<sup>rd</sup> Congress of Pathologies and Rehabilitation of Buildings.
- Laefer, D., Boggs, J., Cooper, N., (2004), “Engineering properties of historic brick – variability considerations as a function of stationary versus nonstationary kiln type.” *Journal of the American Institute of Conservation of Historic and Artistic Work*, 4(3): 255-272.
- Lindmark, S., (1996) “A hypothesis on the mechanism of surface scaling due to combined salt- and frost attack” Report TVBM-7104 presented at RILEM TC 117 meeting, Helsinki, Finland.
- Litvan, G. (1975a). Testing the Frost Susceptibility of Bricks. In *Masonry: Past and Present*, pp. 123–132. ASTM STP 589.
- Litvan, G., (1975b) “Phase Transitions of Adsorbates: VI, Effect of Deicing Agents on the Freezing of Cement Paste”, *Journal of The American Ceramic Society*, 58:1-2 pp.26-30.
- Lstiburek, J.W. (May 2007a). “Building Sciences: The Perfect Wall.” *ASHRAE Journal* (vol. 49); pp. 74-78. Atlanta, GA: American Society of Heating, Refrigeration, and Air-Conditioning Engineers, Inc.
- Lstiburek, J. (July 2007b). “Building Sciences: Capillary Suction-Small Sacrifices.” *ASHRAE Journal*, (vol. 49); pp. 58-61). Atlanta, GA: American Society of Heating, Refrigeration, and Air-Conditioning Engineers, Inc.
- Lstiburek, J. (August 2008). “Building Sciences: Energy Flow Across Enclosures.” *ASHRAE Journal*, (vol. 50); pp. 60-65). Atlanta, GA: American Society of Heating, Refrigeration, and Air-Conditioning Engineers, Inc.
- Lstiburek, J.W. (May 2010). “Building Sciences: Thick as a Brick.” *ASHRAE Journal* (vol. 52); pp. 50-56. Atlanta, GA: American Society of Heating, Refrigeration, and Air-Conditioning Engineers, Inc.

- Maurenbrecher, A.H.P., Shirliffe, C.J., et al. (1998). "Monitoring the Hygrothermal Performance of a Masonry Wall with and Without Thermal Insulation." *Proceedings of the 8th Canadian Masonry Symposium* (Jasper, Alberta) pp. 174-193, (NRCC-42462).
- Mensinga, P., J. Straube, C. Schumacher. (2010). "Assessing the Freeze-Thaw Resistance of Clay Brick for Interior Insulation Retrofit Projects" *Performance of the Exterior Envelopes of Whole Buildings XI*. Atlanta, GA: American Society of Heating, Refrigeration, and Air-Conditioning Engineers, Inc.
- Morelli, M. (2010). "Internal Insulation of Masonry Walls with Wooden Floor Beams in Northern Humid Climate" *Performance of the Exterior Envelopes of Whole Buildings XI*. Atlanta, GA: American Society of Heating, Refrigeration, and Air-Conditioning Engineers, Inc.
- Morelli, M. and Svendsen, S. (2012) "Investigation of Interior Post-Insulated Masonry Walls with Wooden Beam Ends." *Journal of Building Physics*, June 2012 0(0) 1–29. Thousand Oaks, CA: SAGE Publications.
- [NPS] National Park Service (Preservation Assistance Division). (1984) "A Glossary of Historic Masonry Deterioration Problems and Preservation Treatments." Washington, DC: United States Department of the Interior.
- Ottosen, L., Pederson, A., Roter-Dalgaard, I., (2007) "Salt-related problems in brick masonry and electrokinetic removal of salts" *Journal of Building Appraisal* 3(3) pp. 181-194.
- Perry, S., Duffy, A., (1997) "The short-term effects of mortar joints on salt movement in Stone", *Atmospheric Environment* 31(9) p.p.1297-1305.
- Pigeon, M. and Pleau, R., (1995). *Durability of Concrete in Cold Climates*, Modern Concrete Technology 4, E & FN Spon, New York, NY.
- Scheffler, G.A. (2009). "Moisture Problems at Wooden Beam Ends after Building Renovation." LavEByg conference om strategi for lavenergirenovering, 22. April 2009, Hørsholm, Denmark.
- Schumacher, C.J. (2011). "Assessing the Freeze-Thaw Resistance of Clay Brick for Interior Insulation Retrofit Projects." Interior Insulation Retrofit of Mass Masonry Wall Assemblies Workshop, Westford, MA - July 30, 2011. [http://www.buildingscienceconsulting.com/services/documents/file/2011-07-30%20Schumacher%20Assessing%20FT%20Resistance\\_s.pdf](http://www.buildingscienceconsulting.com/services/documents/file/2011-07-30%20Schumacher%20Assessing%20FT%20Resistance_s.pdf)
- Straube, J.F., Onysko, D., and Schumacher, C.J. (2002). "Methodology and Design of Field Experiments for Monitoring the Hygrothermal Performance of Wood Frame Enclosures," *Journal of Thermal Env. & Bldg. Sci.*, Vol.26, No.2—October 2002. Thousand Oaks, Calif.: SAGE Publications.
- Straube, J.F., and Schumacher, C.J. (2002). "Comparison of Monitored and Modeled Envelope Performance for a Solid Masonry Building." CMHC Report 63204, Ottawa, ON.
- Straube, J.F., and Schumacher, C.J. (2004). "Hygrothermal Modeling of Building Envelopes Retrofits." CMHC Report, Ottawa, ON.

Straube, J.F., and Burnett, E.F.P., (2005). *Building Science for Building Enclosure Design*, Building Science Press: Somerville, MA.

Straube, J.F. and C.J. Schumacher. (2007). "Interior Insulation Retrofits of Load-Bearing Masonry Walls in Cold Climates." *Journal of Green Buildings* 2(2):42–50.

Ueno, K., and Straube J. (2008) "Laboratory Calibration and Field Results of Wood Resistance Humidity Sensors", *Proceedings of BEST 1 Conference*, Minneapolis, June 10-12, 2008.

Ueno, K. (2012) "Masonry Wall Interior Insulation Retrofit Embedded Beam Simulations." *Proceedings of BEST 3 Conference*, Atlanta, GA, April 2 - 4, 2012.

Verbeck, G. J., and Klieger, P., (1957) "Studies of 'Salt' Scaling of Concrete," *Bulletin No. 150*, Highway (Transportation) Research Board, Washington, DC, pp. 1-13.

Wessman, L., (1997) "Studies on the frost resistance of natural stone." Div. of Building Materials, Lund Institute of Technology, Report TVBM-3077, Lund.

Woolfitt, C., (2000), "Soluble Salts in Masonry" *The Building Conservation Directory*. Cathedral Communications Limited, Wiltshire, UK.

*buildingamerica.gov*

U.S. DEPARTMENT OF  
**ENERGY** | Energy Efficiency &  
Renewable Energy

DOE/GO-000000-0000 • Month Year

Printed with a renewable-source ink on paper containing at least 50% wastepaper, including 10% post-consumer waste.

## **BA-1307: Interior Insulation of Mass Masonry Walls: Joist Monitoring, Material Test Optimization, Salt Effects**

### **About this Report**

This report was prepared with the cooperation of the U.S. Department of Energy's Building America Program.

### **About the Authors**

**Kohta Ueno** is a Senior Associate at Building Science Corporation.

Direct all correspondence to: Building Science Corporation, 30 Forest Street, Somerville, MA 02143.

### **Limits of Liability and Disclaimer of Warranty:**

Building Science documents are intended for professionals. The author and the publisher of this article have used their best efforts to provide accurate and authoritative information in regard to the subject matter covered. The author and publisher make no warranty of any kind, expressed or implied, with regard to the information contained in this article.

The information presented in this article must be used with care by professionals who understand the implications of what they are doing. If professional advice or other expert assistance is required, the services of a competent professional shall be sought. The author and publisher shall not be liable in the event of incidental or consequential damages in connection with, or arising from, the use of the information contained within this Building Science document.